

AD \_\_\_\_\_

Award Number: DAMD17-99-1-9088

TITLE: Identification and Characterization of Novel Antimitotic  
Compounds for the Treatment of Breast Cancer

PRINCIPAL INVESTIGATOR: Michel Roberge, Ph.D.

CONTRACTING ORGANIZATION: The University of British Columbia  
Vancouver, BC V6T 1Z3

REPORT DATE: August 2000

TYPE OF REPORT: Annual

PREPARED FOR: U.S. Army Medical Research and Materiel Command  
Fort Detrick, Maryland 21702-5012

DISTRIBUTION STATEMENT: Approved for Public Release;  
Distribution Unlimited

The views, opinions and/or findings contained in this report are those of the author(s) and should not be construed as an official Department of the Army position, policy or decision unless so designated by other documentation.

# REPORT DOCUMENTATION PAGE

Form Approved  
OMB No. 074-0188

Public reporting burden for this collection of information is estimated to average 1 hour per response, including the time for reviewing instructions, searching existing data sources, gathering and maintaining the data needed, and completing and reviewing this collection of information. Send comments regarding this burden estimate or any other aspect of this collection of information, including suggestions for reducing this burden to Washington Headquarters Services, Directorate for Information Operations and Reports, 1215 Jefferson Davis Highway, Suite 1204, Arlington, VA 22202-4302, and to the Office of Management and Budget, Paperwork Reduction Project (0704-0188), Washington, DC 20503

1. AGENCY USE ONLY (Leave blank)

2. REPORT DATE  
August 2000

3. REPORT TYPE AND DATES COVERED  
Annual (15 Jul 99 - 15 Jul 00)

4. TITLE AND SUBTITLE  
Identification and Characterization of Novel Antimitotic Compounds for the Treatment of Breast Cancer

5. FUNDING NUMBERS  
DAMD17-99-1-9088

6. AUTHOR(S)  
Michel Roberge, Ph.D.

7. PERFORMING ORGANIZATION NAME(S) AND ADDRESS(ES)  
The University of British Columbia  
Vancouver, BC V6T 1Z3

8. PERFORMING ORGANIZATION  
REPORT NUMBER

E-MAIL:  
michel@otter.biochem.ubc.ca

9. SPONSORING / MONITORING AGENCY NAME(S) AND ADDRESS(ES)

U.S. Army Medical Research and Materiel Command  
Fort Detrick, Maryland 21702-5012

10. SPONSORING / MONITORING  
AGENCY REPORT NUMBER

11. SUPPLEMENTARY NOTES

12a. DISTRIBUTION / AVAILABILITY STATEMENT  
Approved for public release; distribution unlimited

12b. DISTRIBUTION CODE

13. ABSTRACT (*Maximum 200 Words*)

Our goal is to find new antimitotic drugs for the treatment of breast cancer using a novel cell-based assay to screen natural product libraries and guide the purification of their active components.

We have completed a screen of over 30,000 extracts of terrestrial plants, algae and marine organisms and obtained 223 positive extracts. To maximize our chance of finding novel and useful compounds, we have carried out a variety of different tests on the positive extracts and prioritized for further study those that are particularly potent, those that are particularly effective against multidrug-resistant breast cancer cells, those that cause microtubule bundling, those that come from unusual or little-studied organisms, and those that appear to act by unusual mechanisms.

We have purified and studied the active compounds from 5 of these positive extracts and a further 17 are undergoing purification. Our screen also revealed a new source of eleutherobin. This promising compound was discovered in 1997 but lack of material impeded its development. Our source is abundant and may provide sufficient material for preclinical and early phase clinical trials. We also discovered novel eleutherobin analogs, carried out a structure-activity study, and determined the solution and crystal structures of eleutherobin, all of which will be important for drug development.

We are confident that year 2 will proceed as scheduled and that of our 223 positive extracts some will yield structurally novel compounds that will be useful lead compounds for therapy.

14. SUBJECT TERMS  
Breast Cancer

15. NUMBER OF PAGES

51

16. PRICE CODE

17. SECURITY CLASSIFICATION  
OF REPORT  
Unclassified

18. SECURITY CLASSIFICATION  
OF THIS PAGE  
Unclassified

19. SECURITY CLASSIFICATION  
OF ABSTRACT  
Unclassified

20. LIMITATION OF ABSTRACT  
Unlimited

NSN 7540-01-280-5500

Standard Form 298 (Rev. 2-89)  
Prescribed by ANSI Std. Z39-18  
298-102

## Table of Contents

Cover.....	1
SF 298.....	2
Table of Contents.....	3
Introduction.....	4
Body.....	4
Key Research Accomplishments.....	8
Reportable Outcomes.....	10
Conclusions.....	10
References.....	10
Appendices.....	11

## INTRODUCTION

Antimitotics are drugs that kill cancer cells by causing them to arrest in mitosis. Antimitotics currently used in breast cancer therapy include paclitaxel, vincristine and vinblastine. Although these drugs are extremely valuable, they are not ideal because they have serious side effects, and, most importantly, many breast cancers are resistant to them. Our goal is to find new antimitotic drugs for the treatment of breast cancer using a novel cell-based assay to screen natural product libraries and guide the purification of their active components.

## BODY

### TASK 1

Screen the natural product collection (5,000 extracts) for antimitotic activity (months 1-4)

We have completed a major screen of about 30,000 extracts. In addition to the proposed collection of marine microorganisms, we have also screened two other collections in order to maximize the diversity of sources of antimitotics. One was of marine invertebrates collected by the Andersen laboratory from a variety of habitats: cold temperate Pacific Ocean waters along the coast of British Columbia, tropical Pacific Ocean reefs off Motupore and Madang in Papua New Guinea, tropical waters off the island of Dominica in the Caribbean, and temperate Atlantic waters surrounding the Isle of Man (U.K.). The second collection was obtained from the Natural Products Repository of the National Cancer Institute Developmental Therapeutics Program. It is a diverse collection of terrestrial plants, algae and marine organisms from around the world. Access to this valuable collection was granted in January 1999.

The screen has certainly lived up to our expectations. The pilot study we presented in our proposal yielded two antimitotics out of 263 screened, a hit rate of 0.7%. Our final screen has given us 223 positive extracts out of 30,000 screened, also a hit rate of 0.7%.

To deal with the massive amount of screening we adapted our original assay. The ELISA (described in detail in the proposal) is a moderately lengthy and labor-intensive procedure requiring the preparation of cell lysates, their transfer to protein-binding plates, and many solution changes. We have subsequently simplified it, reducing the time of the procedure and the number of steps by half and avoiding transfer of samples to ELISA plates. This also reduces the use of materials. In the new procedure, the cells are fixed with formaldehyde in the microtiter culture plate and permeabilized with methanol and detergents, and the TG-3 primary antibody and HRP-conjugated secondary antibody are added simultaneously. Colorimetric detection of HRP activity remains unchanged. Since cell fixation and permeabilization *in situ* are steps commonly used in immunocytochemistry, we termed the assay Enzyme-Linked Immuno-Cytochemical Assay or ELICA.

A manuscript describing the original ELISA assay and the modified ELICA assay, and the screen of the first 25,000 extracts has been accepted for publication in Cancer Research. A copy (Roberge et al., 2000) is provided in Appendix 1. This manuscript also describes the purification and characterization of the active compounds from 5 positive extracts, described under later Tasks.

In order to handle the large amount of data being generated by our screen, we have developed a database for all the positive extracts. The database lists each extract's date of screening, its storage location, identifying number, its source (marine invertebrate, plant, or alga), its family, genus and species, and notes concerning the stage of purification and/or characterization it has undergone. The database may be searched by any of these parameters. An example of part of our database is shown overleaf.

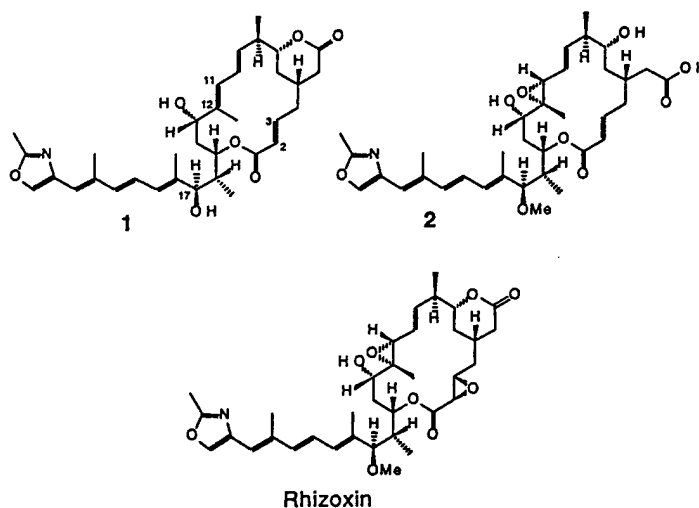
Plate #	Well	Code	Source	Genus	Species	Family	Comments
970201 17	E05	N29 701	Plant	Ilex	macrophylla	Aquifoliaceae	Completed: B. Cinel - paclitaxel analogs
970401 40	G10	N79 009	Plant	Ilex	sideroxyloides	Aquifoliaceae	paclitaxel?
970401 54	A05	N71 889	Plant	Combretum	fuscum	Combretaceae	combretastatin?

We have found the database to be particularly useful when prioritizing extracts to undergo chemical purification. For example, positive extracts from organisms of the same genus, such as the plants *Ilex sideroxyloides* and *Ilex macrophylla* are very likely to contain the same or similar antimicrobials. Only one would be selected for further intensive study when searching for structurally novel compounds. Similarly extracts from organisms in the same genus as an organism known to contain an identified antimicrobially active compound would be a low priority for further study. For example, the positive extract of *Combretum fuscum* is very likely to contain the known antimicrobially active compound combretastatin originally identified in *Combretum caffrum* [Sackett, 1993]. The other side of the coin is that in order to find new analogs of a particularly important antimicrobially active compound, extracts from related organisms may be selected. We have taken this approach for finding new analogs of eleutherobin, and selected extracts from organisms related to *Erythropodium caribaeorum* for further study. The significance of this choice is detailed under Task 2.

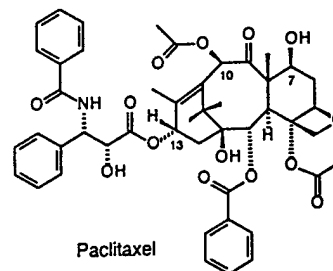
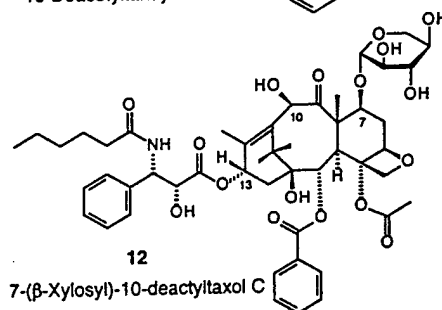
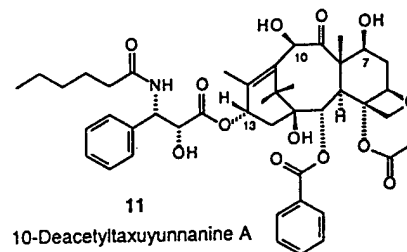
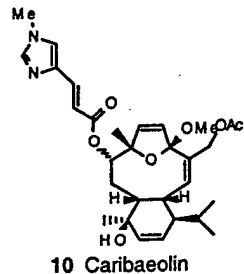
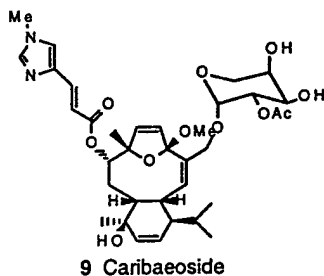
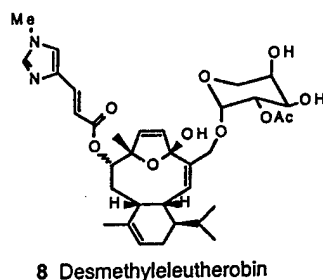
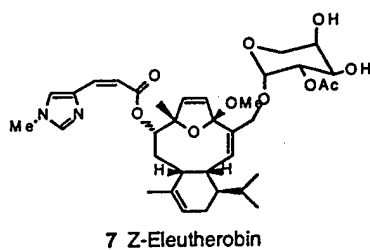
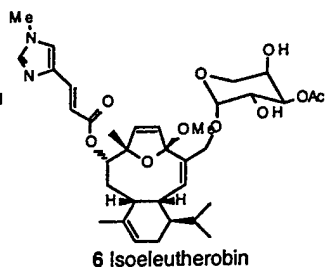
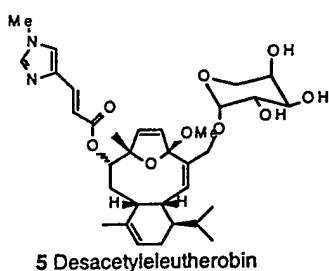
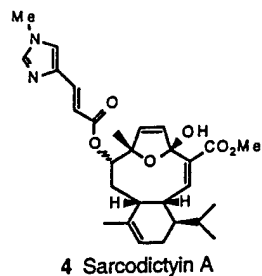
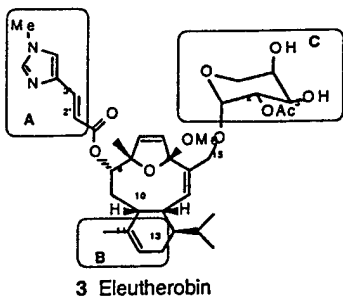
## TASK 2

Isolate and identify the chemical structure of active compounds (months 5-30)

We have completed the process of fractionation, dereplication, purification and chemical structure elucidation of active compounds for five positive extracts. These results are described in the manuscript Roberge et al., 2000 and published paper Cinel et al., 2000a, both provided in Appendix 1. We found a new rhizoxin analog from a *Pseudomonas* species, six new eleutherobin analogs from the octocoral *Erythropodium caribaeorum*, and two paclitaxel analogs in the stem bark of the tree *Ilex macrophylla*. Their structural formulae are shown below.



Structural formulae of rhizoxin and analogs (1-2) purified from *Pseudomonas* sp.



Structural formulae of eleutherobin and analogs (3-10) purified from *Erythropodium caribaeorum*, and paclitaxel and analogs (11-12) purified from *Ilex macrophylla*

In addition, we have been able to use our assay to quantitatively compare the antimittotic activity of the different analogs of rhizoxin, eleutherobin, and paclitaxel, permitting us to determine which regions of these compounds are important for antimittotic activity. This information is very useful for further drug development. The results are described in Roberge et al., 2000 and Cinel et al., 2000a (Appendix 1). We have also been able to determine the solution and crystal structures of eleutherobin. This is important for understanding which regions of the molecule are important for activity and also for developing a general pharmacophore for how microtubule-bundling agents work. The results are described in Cinel et al., 2000b (Appendix 1).

An additional 17 extracts are at various stages of chemical investigation, insufficient material having stopped the further investigation of an 18th. Of these, twelve are extracts

from sponges related to *E. caribaeorum* that we suspect might contain additional eleutherobin analogs and are currently at an advanced stage of examination. Eleutherobin raised a considerable amount of interest when it was discovered in 1997 but lack of a suitable source has prevented further development. A comparative study of the potency of different analogs and of sources of eleutherobin will be extremely useful for selecting a compound and suitable source for preclinical evaluation of this promising agent.

Two extracts which were particularly active against multidrug-resistant cells (see Task 4 below) are in the early stages of purification.

A 15th extract has been fractionated and dereplicated and contains no known antimitotic. An investigation of its possible mechanism of action (see Task 3 below), using tubulin immunofluorescence showed that it causes neither tubulin depolymerization, like the vinca alkaloids, nor polymerization, like paclitaxel. Rather its effects were like those we observed some years ago with the drug fostriecin which we subsequently showed to be a protein phosphatase inhibitor. We predicted that our screen might reveal this kind of compound. Further biochemical testing of the extract has confirmed that it does contain a protein phosphatase inhibitor but dereplication indicates that its structure is unlike those currently known. Its final purification is now underway.

A 16th extract is also at the late stages of purification, and a 17th is at the initial fractionation stage.

### **TASK 3**

#### Mechanism of action of new antimitotic compounds (months 13-32)

This task was originally assigned to commence in year 2, using purified antimitotics. However, the large number of positive extracts obtained through the screen prompted us to bring forward the investigation of their probable mechanism of action in order to prioritize them for further study. The use of the crude extracts rather than the purified compounds does not always permit a conclusive result since extracts may contain components somewhat toxic to cells, resulting in abnormal morphology or poor growth. However, in many cases the results were very useful. Final elucidation of mechanism of action will proceed later with the purified compounds, as proposed initially.

Cells grown on coverslips were treated with positive extracts and examined by immunofluorescence microscopy using a monoclonal antibody to  $\beta$ -tubulin and the DNA dye bisbenzimidazole. Two extracts that gave distinct microtubule bundling, a characteristic of paclitaxel, were selected for further investigation and subsequently yielded eleutherobin analogs and paclitaxel analogs, described in Roberge et al., 2000 and Cinel et al., 2000a (Appendix 1). Another extract giving no tubulin bundling or depolymerization but a morphology very like that we have observed for the protein phosphatase inhibitor fostriecin was also selected for further study and has been confirmed to contain a protein phosphatase inhibitor whose structure is unlike those currently known. Its purification is ongoing.

### **TASK 4**

#### Initial studies on therapeutic potential (months 14-36)

As for task 3 above, this task was originally assigned to year 2 to study purified antimitotics, but was brought forward in order to prioritize extracts for further study.

We examined the cytotoxicity of each positive extract to MCF-7 breast carcinoma cells and to multidrug-resistant MCF-7 cells. The same caution for working with extracts rather than purified compounds applied above to Task 3 also applies here: extracts may contain components other than the antimitotic that are toxic to cells. Nevertheless, we found the assay worked well with some extracts, permitting us to select two that were particularly cytotoxic to multidrug-resistant cells. Their purification is ongoing.

## KEY RESEARCH ACCOMPLISHMENTS

- We have developed the ELICA, a modification of our original assay, which is faster, less labor-intensive and less costly.
- We have been able to dramatically increase the diversity of our antimetabolic screen over that in our original proposal because, in January 1999, we were selected by the National Cancer Institute to screen extracts in the Open Repository of their Natural Products Repository. An additional collection of marine organisms was also made available by Dr R.J. Andersen. We have completed a screen of some 30,000 extracts of plants, algae and marine organisms and obtained 223 positives. Our overall rate of 0.7% positives is as predicted from the pilot study presented in our proposal. However, we find that among the different sources of extracts tested, marine organisms tend to show the greatest proportion of positives.
- We have developed a database for the positive extracts, listing their date of screening, location, identifying number, source, family, genus, and species.
- To prioritize extracts for the lengthy and difficult process of purification and structure elucidation, we have subjected them to a variety of tests originally planned for use with purified extracts in years 2 and 3. Each positive extract was studied for its potency in mitotic arrest, its potential mechanism of action (whether it caused microtubule bundling, microtubule depolymerization or acted by another mechanism), and its activity against multidrug-resistant breast cancer cells. In addition we evaluated the phylogenetic relationship of the source of the extract to other species containing known antimetabolites.
- We have completed the purification and identification of active compounds from five positive extracts, including analogs of rhizoxin, eleutherobin and paclitaxel. A further 17 extracts are at various stages of purification. They were selected because they are particularly potent, cause microtubule bundling, are particularly effective against multidrug-resistant breast cancer cells, act by unusual mechanisms, come from unusual or little-studied organisms, or come from organisms we believe may contain valuable analogs of known antimetabolites.
- An unexpected outcome of our screen is that although the active compounds whose purification and structural elucidation we have completed belong to known antimetabolic chemotypes, they were found in organisms not known or suspected to produce them. Our finding of eleutherobin in *E. caribaeorum* is of particular significance because eleutherobin was originally found in the Australian soft coral *Eleutherobia* and it has not been possible to obtain sufficient amounts for preclinical development [Rayl, 1999]. Although eleutherobin has been synthesized by several research groups, the amounts obtained are insufficient for development. In contrast *E. caribaeorum* is widespread in the Caribbean and has been grown in aquaria and may thus constitute a suitable source of eleutherobin for preclinical and early phase clinical trials.
- An important outcome of our screen is that our assay has permitted us to detect antimetabolic agents in extracts that were previously studied but not found to contain them by other methods. *E. caribaeorum* has been subjected to extensive chemical characterization [Look, 1984] but eleutherobin compounds were not detected because they are very minor components. The COMPARE algorithm, which is able to detect similar differential patterns of growth inhibition for the 60 human cell lines in the NCI anticancer drug screen, has been used successfully to identify new antimetabolic agents from the NCI collection of pure compounds [Paull, 1992]. When used with the crude

plant extracts in the Natural Products Repository, a COMPARE analysis using paclitaxel as the probe identified 47 extracts with a Pearson correlation coefficient above 0.6. Three of these were also positive in our antimitotic screen and all three were from *Catharanthus roseus*, the plant from which the vinca alkaloids were originally isolated. The analysis did not identify the extract of *Ilex macrophylla* from which we isolated eleutherobin analogs. This illustrates the usefulness of our cell-based assay for the identification of active compounds present in very low abundance in crude natural extracts.

- We have used our assay to compare quantitatively the antimitotic activity of different analogs of rhizoxin, paclitaxel and eleutherobin, which provides important structural information for further drug development. We have also determined the solution and crystal structure of eleutherobin which is important for determining how microtubule-bundling agents work.

## REPORTABLE OUTCOMES

### Manuscripts (copies provided in Appendix 1)

1. Roberge M, Cinel B, Anderson HJ, Lim L, Jiang X, Xu L, Bigg CM, Kelly MT and Andersen RJ. Cell-based screen for antimetabolic agents and identification of analogs of rhizoxin, eleutherobin and paclitaxel in natural extracts. *Cancer Res.* (in press)
2. Cinel B, Roberge, M. Behrisch, H. and van Ofwegen, L (2000a). Antimetabolic diterpenes from *Erythropodium caribaeorum* test pharmacophore models for microtubule stabilization. *Org. Lett.* 2, 257-260.
3. Cinel B, Patrick BO, Roberge M and Andersen RJ (2000b). Solid-state and solution conformations of eleutherobin obtained from X-ray diffraction analysis and solution NOE data. *Tetrahedron Letters* 41, 2811-2815.

### Patents

Canadian Patent Application filed November 24, 1999: Novel Source of Eleutherobin and related Antimetabolic Diterpenes

## CONCLUSIONS

Our cell-based assay for antimetabolites has met all the expectations we had following our pilot study. We have accomplished all our goals for year 1 of the grant, having completed screening of our extract libraries and completed the purification and structure elucidation of active components from five positive extracts and commenced this process for a further 17. We have also begun tasks assigned to years 2 and 3, the determination of mechanism of action and assessment of therapeutic potential.

Of immediate value to breast cancer treatment is that our research has revealed a new source of the compound eleutherobin which should provide sufficient material for preclinical and early phase clinical trials of this promising compound. We have also provided information about eleutherobin that will be useful for further development as a drug: its crystal and solution structures, and structure-activity relationships using the different analogues we have purified.

We are confident that year 2 will proceed as scheduled and that some of our 223 positive extracts will yield structurally novel compounds that will be useful lead compounds for therapy.

## REFERENCES

- Look SA, Fenical W, van Engen D and Clardy J (1984). Erythrolides: unique marine diterpenoids interrelated by a naturally occurring Di- $\pi$ -methane rearrangement. *J. Am. Chem. Soc.* 106, 5026-5027.
- Paull KD, Lin CM, Malspeis L and Hamel, E (1992). Identification of novel antimetabolic agents acting at the tubulin level by computer-assisted evaluation of differential cytotoxicity data. *Cancer Res.* 52, 3892-3900.
- Rayl AJS (1999). Oceans: medicine chests of the future? *The Scientist* 13, 1-5.
- Sackett DL (1993). Podophyllotoxin, steganacin and combretastatin: natural products that bind at the colchicine site of tubulin. *Pharmacol. Ther.* 59, 163-228.

**APPENDIX 1**

Manuscripts and published papers arising from research carried out in year 1 of this grant.

**Cell-based screen for antimetabolic agents and identification of analogs of rhizoxin, eleutherobin and paclitaxel in natural extracts<sup>1</sup>**

Michel Roberge<sup>2</sup>, Bruno Cinel, Hilary J. Anderson, Lynette Lim, Xiuxian Jiang, Lin Xu, Cristina M. Bigg, Michael T. Kelly and Raymond J. Andersen

Department of Biochemistry and Molecular Biology, University of British Columbia, Vancouver, British Columbia, Canada V6T 1Z3 [M. R., H. J. A., L. L., X. J., C.M.B.], Departments of Chemistry and Oceanography (EOS), University of British Columbia, Vancouver, Canada V6T 1Z1 [B. C., L. X., R. J. A.], and SeaTek Marine Biotechnology Inc., Surrey, British Columbia, Canada, V4A 7M4 [M. T. K.]

Running title: Screen for antimetabolic agents

Keywords: antineoplastic agent, drug discovery, microtubule, small molecule inhibitors, TG-3 monoclonal antibody

Footnotes:

<sup>1</sup>Supported by the Canadian Breast Cancer Research Initiative and the U.S. Department of Defense Breast Cancer Research Program Idea Award # DAMD17-99-1-9088 (M. R.) and the National Cancer Institute of Canada (R. J. A.)

<sup>2</sup>To whom requests for reprints should be addressed, at Department of Biochemistry and Molecular Biology, University of British Columbia, 2146 Health Sciences Mall, Vancouver, B.C., Canada V6T 1Z3. Phone: (604) 822-2304; Fax: (604) 822-5227; E-mail: michel@otter.biochem.ubc.ca.

<sup>3</sup>The abbreviations used are: DMSO, dimethylsulfoxide; ELISA, enzyme-linked immunosorbent assay; ELICA, enzyme-linked immuno-cytochemical assay; HRP, horseradish peroxidase; NCI, National Cancer Institute

## ABSTRACT

We describe a cell-based assay for antimetabolic compounds that is suitable for drug discovery and for quantitative determination of antimetabolic activity. In the assay, cells arrested in mitosis as a result of exposure to antimetabolic agents in pure form or in crude natural extracts are detected by ELISA using the monoclonal antibody TG-3. The assay was used to screen over 24,000 extracts of marine microorganisms and invertebrates and terrestrial plants, and to guide the purification of active compounds from five of 119 positive extracts. A new rhizoxin analog was found in a *Pseudomonas* species, six new eleutherobin analogs were identified from the octocoral *Erythropodium caribaeorum*, and two paclitaxel analogs were found in the stem bark of the tree *Ilex macrophylla*. The assay was also used for quantitative comparison of the antimetabolic activity of different analogs. It revealed the importance of the C-11 to C-13 segment of the diterpene core of eleutherobin for its antimetabolic activity. The identification of antimetabolic compounds in very low abundance and their high (0.5%) occurrence in natural extracts indicates that drug discovery efforts using this cell-based assay may lead to the identification of structurally novel antimetabolic agents.

## INTRODUCTION

Antimitotic agents are compounds that arrest cells in mitosis. Several are clinically important anticancer drugs, including the vinca alkaloids vinblastine, vincristine, and vinorelbine (1) and the taxanes paclitaxel and docetaxel (2). They cause mitotic arrest by interfering with the assembly or disassembly of  $\alpha$ - and  $\beta$ -tubulin into microtubules. At high concentrations, the vinca alkaloids and most other antimitotics cause complete microtubule depolymerization, whereas the taxanes cause bundling of microtubules by stabilizing them against depolymerization. At low concentrations, neither depolymerization nor bundling is observed, but there is sufficient alteration in the dynamics of tubulin loss or addition at the ends of mitotic spindle microtubules to prevent the spindle from carrying out its function of attaching to and segregating the chromosomes, and cells arrest in mitosis (3, 4). Prolonged arrest eventually leads to cell death, either in mitosis or after an eventual escape from mitotic arrest (5, 6). Another class of antimitotic agents, represented by estramustine, does bind tubulin (7) but may also bind microtubule-associated proteins and prevent them from regulating interactions between tubulin polymers (8). Agents that are not known to interact with microtubules, such as inhibitors of protein phosphatases 1 and 2A and mitotic kinesin inhibitors, can also arrest cells in mitosis (9-11).

The vinca alkaloids were isolated from the periwinkle plant, which originally attracted attention because of reported hypoglycemic properties. However, periwinkle extracts showed no antidiabetic action but were found to prolong the life of mice bearing a transplantable lymphocytic leukemia (1). This led to the identification of vincristine and vinblastine. Paclitaxel was isolated from the bark of the Pacific yew tree, an extract of which showed antineoplastic activity in the NCI<sup>3</sup> large-scale screen (2). Vinorelbine and docetaxel are semisynthetic analogs.

These drugs, while extremely valuable, are not ideal. They have numerous toxicities, principally myelosuppression and neurotoxicity. More importantly, many cancers are inherently resistant to these drugs or become so during prolonged treatment (1, 2). This is often the result of multi-drug resistance caused by overexpression of P-glycoprotein, which functions as a drug efflux pump. Other sources of resistance include increased expression of tubulin isotypes to which

a particular drug binds less effectively, and alterations in  $\alpha$ - and  $\beta$ -tubulin structure, by mutation or posttranslational modification, that reduce binding.

Antimitotics with different chemical structures might show increased specificity to mitotic microtubules rather than neuronal microtubules and reduce unwanted side effects, and might be effective against resistant cancers. Many other antimitotics have been discovered, some of which show promise in preclinical studies or have entered clinical trials (12). However, they were discovered either by serendipity or by cytotoxicity screening, or because they showed patterns of cytotoxic activity against panels of cancer cell lines similar to patterns shown by other antimitotic agents (13). The search for better antimitotics would be greatly aided by rational assays for use in drug screens.

We have developed a rapid and reliable cell-based screen for antimitotic agents. In this paper, we describe the assay, its application to a screen of over 24,000 natural extracts, and the purification and characterization of paclitaxel analogs and new rhizoxin and eleutherobin analogs.

## **MATERIALS AND METHODS**

**Cell culture and treatment.** Human breast carcinoma MCF-7 cells were cultured as monolayers (14). The cells were seeded at 10,000 per well of 96-well polystyrene tissue culture plates (Falcon) in 100  $\mu$ l medium and were allowed to grow overnight. Crude extracts were then added at about 10  $\mu$ g/ml or 1  $\mu$ g/ml, from 1000-fold stocks in DMSO. Untreated samples received an equivalent amount of DMSO and served as negative controls. Cells treated with 100 ng/ml nocodazole (Sigma), from a 1000-fold stock in DMSO, served as positive controls. Cells were incubated for 16-20 h. The relative number of cells in mitosis was then determined by microscopy (14), by ELISA, or by ELICA (see below).

**ELISA of mitotic cells.** After incubation with extracts, the cell culture medium was withdrawn carefully using a pipetor. This did not result in any loss of the rounded-up mitotic cells, which remained attached to the plates. The cells were lysed by adding 100  $\mu$ l of ice-cold lysis buffer (1 mM EGTA pH 7.4, 0.5 mM phenylmethylsulfonyl fluoride) and by pipeting up-and-

down 10 times. The cell lysates were transferred to 96-well PolySorp plates (Nunc) and dried completely in a stream of air at about 37°C from a hair dryer. Vacant protein binding sites were blocked by adding 200 µl per well of antibody buffer (10 mM Tris-HCl pH 7.4, 150 mM NaCl, 0.1 mM phenylmethylsulfonyl fluoride, 3% (w/v) dried nonfat milk (Carnation)) for 1 h at room temperature. This was removed and replaced with 100 µl antibody buffer containing 0.1-0.15 µg/ml TG-3 monoclonal antibody (15, 16). This antibody recognizes a phosphoepitope on nucleolin that is present only at mitosis and was provided by Dr. Peter Davies (Albert Einstein College of Medicine, Bronx, NY). After 16-20 h incubation at 4°C, the antibody solution was removed and the wells were rinsed twice with 200 µl 10 mM Tris-HCl pH 7.4, 0.02% Tween 20. HRP-conjugated goat anti-mouse IgM secondary antibody (Southern Biotechnology Associates) was added at a dilution of 1/500. After overnight incubation at 4°C, the antibody solution was removed and the wells were rinsed 3 times with 200 µl 10 mM Tris-HCl pH 7.4, 0.02% Tween 20. 100 µl of 120 mM Na<sub>2</sub>HPO<sub>4</sub>, 100 mM citric acid, pH 4.0 containing 0.5 µg/ml 2,2'-azino-bis(3-ethylbenzthiazoline-6-sulfonic acid) and 0.01% hydrogen peroxide was added for 1 h at room temperature and absorbance at 405 nm was determined using a Dynex MRX plate reader.

**ELICA of mitotic cells.** After incubation with extracts, the medium was withdrawn carefully using a pipetor and 100 µl of 10 mM Tris-HCl pH 7.4, 150 mM NaCl, containing 3.7% formaldehyde was added to fix the cells for 30 min at 4°C. The fixative was removed and replaced with 100 µl of cold (-20°C) methanol for 5 min to permeabilize the fixed cells. The methanol was removed and the wells were rinsed briefly with 200 µl antibody buffer. Then, 100 µl antibody buffer containing 0.1-0.15 µg/ml TG-3 monoclonal antibody and HRP-conjugated goat anti-mouse IgM secondary antibody at a dilution of 1/500 was added for 16-20 h at 4°C. The plates were washed twice with 200 µl 10 mM Tris-HCl pH 7.4, 0.02% Tween 20. 100 µl of 120 mM Na<sub>2</sub>HPO<sub>4</sub>, 100 mM citric acid, pH 4.0 containing 0.5 µg/ml 2,2'-azino-bis(3-ethylbenzthiazoline-6-sulfonic acid) and 0.01% hydrogen peroxide was added for 1 h at room temperature and absorbance at 405 nm was measured. Additional information about this assay is provided in Results.

**Sample collection and extract preparation.** Approximately 250 g each of marine invertebrates were collected by hand, using scuba, from the cold temperate waters of the Pacific Ocean along the coast of British Columbia, from tropical Pacific Ocean reefs off Motupore and Madang in Papua New Guinea, and from tropical waters off the island of Dominica in the Caribbean. Samples were deep frozen on site and transported to Vancouver over dry ice. Voucher samples of each invertebrate are stored in methanol at  $-20^{\circ}\text{C}$  at the University of British Columbia for taxonomic identification. Marine microorganisms were isolated from the invertebrates on site using various marine culture media, and pure cultures were grown as lawns on solid agar marine media in 10 cm petri plates for several days and then freeze-dried.

Extracts of invertebrates were prepared by homogenizing in methanol approximately 200 g of each sample. The homogenates were filtered and concentrated to dryness *in vacuo* to give a gummy residue. Extracts of microorganisms were prepared by extracting the freeze-dried culture (cells and agar) multiple times with dry methanol/acetone, followed by lyophilization. A small amount of each extract was dissolved in DMSO for the antimutagenic screen. Extracts of terrestrial plants were obtained from the Open Repository Program of the Natural Products Repository of the NCI Developmental Therapeutics Program as 500  $\mu\text{g}$  samples which were dissolved in 100  $\mu\text{l}$  DMSO. All diluted extracts were stored at  $-20^{\circ}\text{C}$ .

## RESULTS

**Screen for antimutagenic agents.** The TG-3 monoclonal antibody, originally described as a marker of Alzheimer's disease (15), is highly specific for mitotic cells. Flow cytometry shows that TG-3 immunofluorescence is  $>50$ -fold more intense in mitotic cells than in interphase cells (16). In western blots, the antibody reacts with a 105-kDa protein that is present in abundance in extracts of cells treated for 20 h with the antimutagenic agent nocodazole but present at only low levels in extracts from cycling MCF-7 cells (Fig. 1). This protein has been identified as a mitotically phosphorylated form of nucleolin (17). Densitometric scanning of the bands showed a 27-fold difference in intensity between nocodazole-treated and untreated cells, corresponding well to the

difference in the number of mitotic cells in the two samples: 80% for the nocodazole-treated sample and 3% for the untreated sample, as measured by microscopy.

TG-3 also recognizes mitotic cells in ELISA using microtiter plates (18). In this standard assay (19), cells grown in 96-well plates are lysed and the lysates are transferred to protein-binding ELISA plates for adsorption to the plastic surface. The antigen is detected by incubating with TG-3 antibody followed by an HRP-conjugated secondary antibody and colorimetric determination of HRP activity.

We first tested the suitability of the ELISA for quantifying the activity of antimetabolic agents. MCF-7 cells were incubated for 20 h with different concentrations of the antimetabolic drug paclitaxel, and the proportion of cells arrested in mitosis was measured by counting mitotic figures in the microscope, and by ELISA. Paclitaxel induced mitotic arrest in a concentration-dependent manner with half-maximal activity at 10 nM measured by microscopy (Fig. 2A) and at 4 nM measured by ELISA (Fig. 2B, open squares).

ELISA is a lengthy and labor-intensive procedure requiring the preparation of cell lysates, their transfer to protein-binding plates, and many solution changes. We subsequently simplified it, reducing the time of the procedure and the number of steps by half and avoiding transfer of samples to ELISA plates. In this procedure, the cells are fixed with formaldehyde in their microtiter culture plate and permeabilized with methanol and detergents, and the TG-3 primary antibody and HRP-conjugated secondary antibody are added simultaneously. Colorimetric detection of HRP activity remains unchanged. Since cell fixation and permeabilization *in situ* are steps commonly used in immunocytochemistry, we termed the assay Enzyme-Linked Immuno-Cytochemical Assay or ELICA.

The ELICA was tested as above. Dose-dependent arrest of cells in mitosis by paclitaxel was detected by ELICA with half-maximal activity at 1.5 nM (Fig. 2, filled squares). The ELICA showed a higher signal at low paclitaxel concentrations and a lower signal at high concentrations than did the ELISA (Fig. 2B). These differences probably resulted from higher non-specific staining of interphase cells because of reduced washing and from lower specific staining of mitotic

cells because of fixation and reduced antibody incubation times. Nevertheless, the ELICA consistently showed sufficient difference in absorbance between cells treated or not with antimetabolic agents to allow unambiguous detection of mitotic cells. Measurements obtained by ELICA consistently showed smaller standard deviations than obtained by ELISA, probably because the reduced number of manipulations reduced experimental variation.

**Screening of natural extracts.** We first tested the suitability of the ELISA for drug screening using a small selection of crude extracts from marine microorganisms (Table 1). Of the 264 extracts tested, 261 showed no activity, giving absorbance readings not statistically different from those of untreated cells. Three extracts clearly showed activity, with absorbance readings of 1.135, 1.437 and 1.245, close to the values obtained with nocodazole as a positive control.

We then screened over 2000 crude extracts of marine sponges, tunicates, soft corals, starfish, and nudibranchs. This screen identified 16 additional extracts with antimetabolic activity. The positive extracts were retested by counting mitotic cells in the microscope and all were confirmed to arrest cells in mitosis.

Finally, we screened crude extracts of terrestrial plants from the NCI Natural Products Repository by ELICA. The suitability of the ELICA for drug screening is illustrated in Table 2, which displays a screen of 264 plant extracts from three randomly selected 96-well plates. Five extracts showed activity, with absorbance readings close to or higher than those obtained with nocodazole. These positive readings were well above those obtained with negative controls or extracts showing no activity. Of 21,600 plant extracts tested in this manner, 100 showed activity, all of which were confirmed to be positive by microscopy.

All positive extracts from marine organisms and most positive extracts from plants were then rescreened using tubulin immunofluorescence microscopy (14) to examine their effects on microtubule structure. We then purified and identified the active agents in the three microbial extracts, in the single marine invertebrate extract that produced paclitaxel-like bundling of microtubules, and in the terrestrial plant extract that showed clearest evidence of microtubule bundling. The other extracts remain to be studied.

**Identification of new rhizoxin analogs.** Marine bacterial isolate MK7020 collected off the coast of British Columbia, was identified as a *Pseudomonas* sp. by gas chromatographic analysis of cellular fatty acids. The active compounds **1** and **2** (Fig. 3) were purified by chromatographic procedures using the ELISA to guide fractionation. The two other microbial extracts were found to be independent isolates of the same *Pseudomonas* species and contained the same active compounds as MK7020.

Compound **1** is identical to WF-1360C (20, 21), a previously reported analog of the antimitotic agent rhizoxin (Fig. 3). Compound **1** showed half-maximal antimitotic activity ( $IC_{50}$ ) at 52 nM, as determined by ELISA (data not shown). Compound **2** is a new  $\delta$ -lactone seco hydroxy acid and had an  $IC_{50}$  of 8 nM (data not shown).

**Identification of new eleutherobin analogs.** An extract of octocoral *Erythropodium cf. caribaeorum* collected from shallow reefs near Dominica showed antimitotic activity and bundling of microtubules. The active compounds **3-10** (Fig. 4) were isolated and their chemical structure was elucidated as described in detail elsewhere (22).

Compound **3** was identified as eleutherobin, a recently discovered antimitotic agent that acts like paclitaxel by stabilizing microtubules (23, 24). Compound **4** was identified as sarcodictyin A (25) and differs from eleutherobin by replacement of the C-15  $\beta$ -linked 2''-O-acetyl-D arabinopyranose side chain of **3** with a methyl ester and replacement of the C-4 methoxyl with a hydroxyl group. Compounds **5-10** have not been previously reported. Desacetyeleutherobin (**5**) retains the arabinose, but not the 2'' acetyl substituent. Isoeleutherobin A (**6**) has an acetyl group at the 3'' position instead of the 2'' position. Z-eleutherobin (**7**) is a geometric isomer of eleutherobin at the C-2' to C-3' double bond of the C-8 N-(6')-methylurocanic acid ester side chain. Desmethyleleutherobin (**8**) differs from eleutherobin by the presence of a hydroxyl instead of a methoxyl at C-4. Caribaeoside (**9**) differs from eleutherobin by the presence of a hydroxyl at C-11 of the tricyclic core, and a double bond at C-12 to C-13 instead of C-11 to C-12, significantly altering the cyclohexene ring. Caribaeolin (**10**) differs from caribaeoside only by the presence of a  $-CH_2OCO-CH_3$  substituent in the C-3 side chain.

The antimitotic activity profile of these compounds determined by ELICA is shown in Fig. 5. Eleutherobin (**4**) had an  $IC_{50}$  of 100 nM. The activity of Z-eleutherobin (**7**) was close, with an  $IC_{50}$  of 250 nM. Desmethyleleutherobin (**8**) and isoeleutherobin A (**6**) were slightly more potent than eleutherobin, with  $IC_{50}$  of 20 nM and 50 nM, respectively. Desacetyeleutherobin (**5**) was slightly less potent, with an  $IC_{50}$  of 400 nM. Sarcodictyin A (**4**) showed lower activity, with an  $IC_{50}$  of 2  $\mu$ M. Caribaeoside (**9**) and caribeolin (**10**) were considerably less potent, with an  $IC_{50}$  of 20  $\mu$ M for both compounds.

**Identification of paclitaxel analogs in a non-*Taxus* species.** NCI Natural Products Repository extract N29701 was obtained from the stem bark of the tree *Ilex macrophylla* in Kalimantan, Indonesia. It showed antimitotic activity and caused bundling of microtubules. The active compounds were isolated and analysed using ELICA and identified as the known paclitaxel analogs 10-deacetylaxuyunnanine A (**11**) and 7- ( $\beta$ -xylosyl)-10-deacetyltaxol C (**12**) (Fig. 6), by analysis of their nuclear magnetic resonance data and comparison with published values (26, 27). Compounds **11** ( $IC_{50}$ , 0.3  $\mu$ M) and **12** ( $IC_{50}$ , 10  $\mu$ M) were much less potent than paclitaxel ( $IC_{50}$ , 1.5 nM).

## DISCUSSION

**Cell-based assay.** We have described a cell-based assay for antimitotic compounds. When searching for therapeutic agents, cell-based assays are particularly valuable compared with cell-free assays because they select not only for activity against a particular target but also for other desirable properties, such as the ability to permeate cells and to retain activity in tissue culture medium and in cells. In one study, over 90% of compounds found on the basis of *in vitro* target-based assays showed no cytotoxic activity because they did not cross the plasma membrane or were degraded rapidly (28). In addition, assays based on measuring arrest of cells in mitosis have the potential to identify not only agents that interact with microtubules, but also agents that cause mitotic arrest by other mechanisms, such as protein phosphatase inhibitors and mitotic kinesin inhibitors (9-11).

The ELISA and the ELICA procedures both allow unambiguous detection of antimittotic activity in crude natural extracts. The ELICA was used for most of the screening described here because it is faster, less labour-intensive and less costly than the ELISA.

Our screen of over 24,000 crude extracts from different natural sources identified unambiguously 119 with antimittotic activity. The absence of false-positive results was confirmed by microscopy, and all five positive crude extracts that were subjected to further study yielded known or novel antimittotic agents; three extracts from the pilot screen contained members of the rhizoxin family, one marine invertebrate extract contained compounds related to eleutherobin, and a tree extract contained paclitaxel analogs.

**Structure-antimittotic activity relationships.** The assay is useful not only for identifying and purifying antimittotics but also for providing a quantitative measure of their antimittotic activity. This is a helpful indicator of a compound's pharmacological potential since it measures not simply the interaction of the compound with its target, as an *in vitro* assay would do, but its ability to interact with its target within a cell. We used it to compare the antimittotic activity of different analogs of rhizoxin, eleutherobin, and paclitaxel.

Rhizoxin is a 16-membered macrolide isolated in 1984 (29) and later found to cause the accumulation of cells in mitosis (30, 31) and to inhibit microtubule assembly (31, 32). Rhizoxin is very cytotoxic to cancer cells *in vitro* or in mice (20, 30), including cell lines resistant to the vinca alkaloids (30). It has been the subject of several phase I and II clinical trials, but results have been disappointing (reviewed in 33). To the best of our knowledge, the seco hydroxy acid **2** was not previously known as a natural product, having been reported in the patent literature only as a semi-synthetic derivative of the corresponding  $\delta$ -lactone. WF-1360C (**1**) was 15-fold less toxic to P388 cells than rhizoxin (20). It differs from rhizoxin by the presence of a hydroxyl group instead of a methoxyl at C-17 and the absence of the two epoxides at C-2 to C-3 and C-11 to C-12. Compound **2** retains the methoxyl and one epoxide but has an open lactone ring. Comparison of the antimittotic activity of WF-1360C ( $IC_{50}$  52 nM) to that of compound **2** ( $IC_{50}$  8 nM) and to published cytotoxicity data for other analogs (20, 32), indicates that a closed lactone ring is not required for

antimitotic activity and that the presence of a methoxyl substituent at C-17 contributes to the high potency of rhizoxin.

Eleutherobin was identified as a compound with paclitaxel-like properties in 1997 (23), but sarcodictyins A-D were the first members of the eleutherobin class of compounds to be identified (25, 34), their paclitaxel-like properties being recognized only later (35). Sarcodictyin A (4) was 20-fold less active than eleutherobin (3), indicating that the C-15  $\beta$ -linked 2''-O-acetyl-D arabinopyranose side chain or the C-4 methoxyl group is important for antimitotic activity. Desmethyleleutherobin (8) was active, showing that it is the C-15 side chain and not the C-4 methoxyl that is required. Desacetyeleutherobin (5) and isoeleutherobin A (6) showed activity similar to eleutherobin, indicating that the acetyl group does not contribute importantly to activity. Therefore, although the sugar moiety is not absolutely required for antimitotic activity, it contributes to the high potency of eleutherobin.

Isomerization of the C-2' to C-3' double bond of the C-8 side chain of Z-eleutherobin (7) had little effect on the antimitotic activity of the compound, showing that the E configuration in eleutherobin is not required for antimitotic activity. Desmethyleleutherobin (8) was the most active of the compounds tested, suggesting that the C-4 hydroxyl might enhance activity through additional hydrogen bonding, or that the C-4 methoxyl somehow hinders the activity of eleutherobin. Caribaeoside (9) was 200-fold less active than eleutherobin, revealing the importance of the C-11 to C-13 segment for antimitotic activity. Caribaeolin (10) differs from caribaeoside (9) only in the C-3 side chain and the activities of these compounds are similar. Likewise, sarcodictyin A differs from desmethyleleutherobin only in the C-3 side chain but its activity is lower than that of desmethyleleutherobin. These data indicate that the C-15 acetyl-D arabinopyranose can be replaced with an acetoxy functionality without significant loss of activity, confirming earlier data with synthetic analogs (36, 37), but not with a methyl ester.

Thirteen synthetic eleutherobin analogs have recently been described and tested in tubulin polymerization and cytotoxicity assays (36-38). Overall, these studies underlined the importance of the C-8 and C-3 side chains for activity, the C-8 side chain being essential and the sugar or another

bulky substituent being needed at C-3 for optimal activity. All of the synthetic analogs retained the original eleutherobin core and therefore provided no information about the importance of segments of the tricyclic core.

Eleutherobin represents one of five chemical structural types known to arrest cells in mitosis by stabilizing microtubules. The other four are paclitaxel, discodermolide, the epothilones and the laulimalides (39-41). Several pharmacophores have been proposed for members of this group (42-44). The latter (44) included eleutherobin and proposed three regions of common overlap between the chemotypes, shown as boxes A, B and C in Fig. 4. Region A of eleutherobin consists of the C-8 side chain, region B encompasses the C-11 to C-13 segment of the tricyclic skeleton, and region C consists of the C-15 substituent. The importance of regions A and C is supported by the published structure-activity data for eleutherobin analogs mentioned above (36-38). Our demonstration that caribaeoside (**9**), which differs from eleutherobin only in region B, shows a 200-fold lower activity demonstrates an important role for this region in antimitotic activity. Further studies will be required to determine whether the reduced antimitotic activity of caribaeoside is due to reduced affinity for tubulin and microtubules, or to factors such as drug uptake, extrusion or metabolism.

Paclitaxel is an approved drug for the treatment of advanced ovarian cancer and metastatic breast cancer. It was originally isolated from *Taxus brevifolia* in 1971 (45). Since then, over 350 related diterpenoids have been isolated from different species of the genus *Taxus* (46), including compounds **11** and **12** described here. Compound **11** differs from paclitaxel in the nature of the N-acyl substituent on the C-13 phenylisoserine side chain and in the absence of the acetyl substituent at C-10. It was less active than paclitaxel, showing that the C-13 and C-10 substituents, although not essential for activity, contribute to the high potency of paclitaxel. Compound **12** further differs from paclitaxel by the presence of a  $\beta$ -xylosyl substituent at C-7. Compound **12** was less active than compound **11** indicating the C-7 substituent also contributes to the potency of paclitaxel.

**Unexpected outcomes.** An unexpected outcome of this study is that although the active compounds we isolated belong to known antimetabolic chemotypes, they were found in organisms not known or suspected to produce them. To our knowledge, rhizoxin compounds have previously only been isolated from the rice seedling blight fungus *Rhizopus chinensis* and unidentified species of the same genus (29). We have now identified rhizoxin analogs in marine bacterial isolates of the genus *Pseudomonas*, which is common in Pacific Northwest waters. Eleutherobin was originally isolated from the soft coral *Eleutherobia* sp. (possibly *E. albiflora*) collected in Western Australia (23). We now identify eleutherobin in the Caribbean octocoral *Erythropodium caribaeorum*. This is of practical significance because it has not been possible to obtain sufficient amounts of natural or synthetic eleutherobin for preclinical development (47). The taxonomic classification of this source was confirmed by the identification of large quantities of the erythrolide diterpenoids characteristic of this species (48). In contrast to *Eleutherobia*, *E. caribaeorum* is widespread in the Caribbean and Florida (49-51), abundant in certain areas, and has been grown in aquaria. It may thus constitute a suitable source of eleutherobin for preclinical and early phase clinical trials. Paclitaxel and analogs have all been isolated from the bark of yew trees (46), from endophytic fungi isolated from the *Taxus* species or *Taxodium distichum* (52, 53), and recently from an epiphytic fungus on the rubiaceaceous plant *Maguireothamnus speciosus* (54). It was surprising to find paclitaxel analogs in the bark of a non-*Taxus* tree. The taxonomic classification of our extract was confirmed by the presence of the triterpenoid glycosides characteristic of the genus *Ilex* (55). It is possible that an endophytic fungus is responsible for their production in *Ilex macrophylla*.

Perhaps the most important outcome of this study is that the assay permitted us to detect antimetabolic agents in extracts that were not found to contain them using other methods. *E. caribaeorum* has been subjected to extensive chemical characterization (48) but eleutherobin compounds were not detected because they are very minor components. The COMPARE algorithm, which is able to detect similar differential patterns of growth inhibition for the 60 human cell lines in the NCI anticancer drug screen, has been used successfully to identify new antimetabolic agents within the NCI chemical repository of pure compounds (13). Extracts in the NCI Natural

Products Repository have also been tested against the NCI cell line panel. A COMPARE analysis using paclitaxel as the probe compound identified 47 plant extracts with a Pearson correlation coefficient above 0.6 (not shown). Three of these extracts were positive in our antimitotic screen and all three were from *Catharanthus roseus*, the plant from which the vinca alkaloids were originally isolated (1). The analysis did not identify the extract from *Ilex macrophylla* whose growth inhibition pattern does not resemble that of paclitaxel and other antimitotic compounds. This illustrates the usefulness of the cell-based assay for the identification of active compounds present in very low abundance in crude natural extracts. The assay should greatly facilitate the discovery and development of novel antimitotic agents and their characterization in the context of living cells.

#### ACKNOWLEDGMENTS

We thank Peter Davies for providing TG-3 antibody, Hans Behrisch and Ross University for logistic support in the Commonwealth of Dominica and Michael Leblanc, David Williams and Robert Britton for collecting *E. caribaeorum*.

## REFERENCES

1. Rowinsky, E. K. and Donehower, R. C. Antimicrotubule agents. *In*: B. A. Chabner and D. L. Longo (eds.), *Cancer Chemotherapy and Biotherapy*, pp. 263-296. Philadelphia: Lippincott-Raven Publishers, 1996.
2. Rowinsky, E. K. The development and clinical utility of the taxane class of antimicrotubule chemotherapy agents. *Annu. Rev. Med.*, 48: 353-374, 1997.
3. Jordan, M. A., Thrower, D., and Wilson, L. Effects of vinblastine, podophyllotoxin, and nocodazole on mitotic spindles. Implications for the role of microtubule dynamics in mitosis. *J. Cell Sci.*, 102: 401-416, 1992.
4. Jordan, M. A., Toso, R. J., Thrower, D., and Wilson, L. Mechanism of mitotic block and inhibition of cell proliferation by taxol at low concentrations. *Proc. Natl. Acad. Sci. USA*, 90: 9552-9556, 1993.
5. Jordan, M. A. and Wilson, L. Microtubules and actin filaments: dynamic targets for cancer chemotherapy. *Current Opin. Cell Biol.*, 10: 123-130, 1998.
6. Torres, K. and Horwitz, S. B. Mechanisms of taxol-induced cell death are concentration-dependent. *Cancer Res.*, 58: 3620-3626, 1998.
7. Panda, D., Miller, H. P., Islam, K., and Wilson, L. Stabilization of microtubule dynamics by estramustine by binding to a novel site in tubulin: a possible mechanistic basis for its antitumor action. *Proc. Natl. Acad. Sci.*, 94: 10560-10564, 1997.
8. Hudes, G. Estramustine-based chemotherapy. *Semin. Urol. Oncol.*, 15: 13-19, 1997.
9. Roberge, M., Tudan, C., Hung, S. M., Harder, K. W., Jirik, F. R., and Anderson, H. Antitumor drug fostriecin inhibits the mitotic entry checkpoint and protein phosphatases 1 and 2A. *Cancer Res.*, 54: 6115-6121, 1994.
10. Cheng, A., Balczon, R., Zuo, Z., Koons, J. S., Walsh, A. H., and Honkanen, R. E. Fostriecin-mediated G2-M-phase growth arrest correlates with abnormal centrosome replication, the formation of aberrant mitotic spindles, and the inhibition of Serine/Threonine protein phosphatase activity. *Cancer Res.*, 58: 3611-3619, 1998.

11. Mayer, T. U., Kapoor, T. M., Haggarty, S. J., King, R. W., Schreiber, S. L., and Mitchison, T. J. Small molecule inhibitor of mitotic spindle bipolarity identified in a phenotype-based screen. *Science*, 286: 971-974, 1999.
12. Jordan, A., Hadfield, J. A., Lawrence, N., J., and McGown, A. T. Tubulin as a Target for Anticancer Drugs: Agents Which Interact with the Mitotic Spindle. *Med. Res Rev.*, 18: 259-296, 1998.
13. Paull, K. D., Lin, C. M., Malspeis, L., and Hamel, E. Identification of novel antimitotic agents acting at the tubulin level by computer-assisted evaluation of differential cytotoxicity data. *Cancer Res.*, 52: 3892-3900, 1992.
14. Anderson, H. J., Coleman, J. E., Andersen, R. J., and Roberge, M. Cytotoxic peptides hemiasterlin, hemiasterlin A and hemiasterlin B induce mitotic arrest and abnormal spindle formation. *Cancer Chemother. Pharmacol.*, 39: 223-226., 1997.
15. Vincent, I., Rosado, M., and Davies, P. Mitotic mechanisms in Alzheimer's disease? *J. Cell Biol.*, 132: 413-425, 1996.
16. Anderson, H. J., deJong, G., Vincent, I., and Roberge, M. Flow cytometry of mitotic cells. *Expt. Cell Res.*, 238: 498-502, 1998.
17. Dranovsky, A., Gregori, L., Schwartzman, A., Vincent, I., Davies, P., and Goldgaber, D. Distribution of nucleolin in Alzheimer's disease and control brains. *Society for Neuroscience Abstracts.*, 27: 2219, 1997.
18. Roberge, M., Berlinck, R. G. S., Xu, L., Anderson, H. J., Lim, L. Y., Curman, D., Stringer, C. M., Friend, S. H., Davies, P., Haggarty, S. J., Kelly, M. T., Britton, R., Piers, E., and Andersen, R. J. High-throughput assay for G2 checkpoint inhibitors and identification of the structurally novel compound isogranulatimide. *Cancer Res.*, 58: 5701-5706, 1998.
19. Perlmann, H. and Perlmann, P. Enzyme-linked immunosorbent assay. *In: J. E. Celis (ed.) Cell Biology - A practical approach, Vol. 2, pp. 322-328. San Diego: Academic Press, 1994.*

20. Kiyoto, S., Kawai, Y., Kawakita, T., Kino, E., Okuhara, M., Uchida, I., H., T., Hashimoto, M., Terano, H., Kohsaka, M., Aoki, H., and Imanaka, H. A new antitumor complex, WF-1360, WF-1360A, B, C, D, E and F. *J. Antibiot. (Tokyo)*, *39*: 762-772, 1986.
21. Iwasaki, S., Namikoshi, M., Kobayashi, H., Furukawa, J., and Okuda, S. Studies on macrocyclic antibiotics. IX. Novel macrolides from the fungus *Rhizopus chinensis*: precursors of rhizoxin. *Chem. Pharm. Bull.*, *34*: 1387-1390, 1986.
22. Cinel, B., Roberge, M., Behrisch, H., and van Ofwegen, L. Antimitotic diterpenes from *Erythropodium caribaeorum* test pharmacophore models for microtubule stabilization. *Org. Lett.*, *2*: 257-260., 2000.
23. Lindel, T., Jensen, P. R., Fenical, W., Long, B. H., Casazza, A. M., Carboni, J., and Fairchild, C. R. Eleutherobin, a new cytotoxin that mimics paclitaxel (Taxol) by stabilizing microtubules. *J. Am. Chem. Soc.*, *119*: 8744-8745., 1997.
24. Long, B. H., Carboni, J. M., Wasserman, A. J., Cornell, L. A., Casazza, A. M., Jensen, P. R., Lindel, T., Fenical, W., and Fairchild, C. R. Eleutherobin, a novel cytotoxic agent that induces tubulin polymerization, is similar to paclitaxel (Taxol). *Cancer Res.*, *58*: 1111-1115., 1998.
25. D'Ambrosio, M., Guerriero, A., and Pietra, F. Sarcodictyin A and Sarcodictyin B, novel diterpenoidic alcohols esterified by (E)-N(1)-methylurocanic acid. Isolation from the mediterranean stolonifer *Sarcodictyon roseum*. *Helv. Chim. Acta*, *70*: 2019-2027, 1987.
26. Morita, H., Gonda, A., Wei, L., Yamamura, Y., Wakabayashi, H., Takeya, K., and Itokawa, H. Four new taxoids from *Taxus cuspidata* var. *nana*. *Planta Medica*, *64*: 183-186. 1998.
27. Senilh, V., Blechert, S., Colin, M., Guenard, D., Potier, F. P., and Varenne, P. Mise en evidence de nouveaux analogues du taxol extraits de *Taxus baccata*. *J. Nat. Prod.*, *47*: 131-137., 1984.
28. Corbett, T., Valeriote, F., LoRusso, P., Polin, L., Panchapor, C., Pugh, S., White, K., Knight, J., Demchik, L., Jones, J., Jones, L., and Lisow, L. In vivo methods for screening

- and preclinical testing. *In*: B. Teicher (ed.) drug development guide, pp. 75-99. Totowa, NJ: Humana Press Inc., 1997.
29. Iwasaki, S., Kobayashi, H., Furukawa, J., Namikoshi, M., Okuda, S., Sato, Z., Matsuda, I., and Noda, T. Studies on macrocyclic lactone antibiotics. VIII. Structure of a phytotoxin "rhizoxin" produced by *Rhizopus chinensis*. *J. Antibiot.*, *37*: 354-362, 1984.
  30. Tsuruo, T., Oh-hara, T., Iida, H., Tsukagoshi, S., Sato, Z., Matsuda, I., Iwasaki, S., Okuda, S., Shimizu, F., Sasagawa, K., Fukami, M., Fukuda, K., and Arakawa, M. Rhizoxin, a macrocyclic lactone antibiotic, as a new antitumor agent against human and murine tumor cells and their vincristine-resistant sublines. *Cancer Res.*, *46*: 381-385, 1986.
  31. Bai, R., Pettit, G. R., and Hamel, E. Dolastatin, a powerful cytostatic peptide derived from a marine animal: inhibition of tubulin polymerization mediated through the vinca alkaloid binding domain. *Biochem. Pharmacol.*, *39*: 1941-1949., 1990.
  32. Takahashi, M., Iwasaki, S., Kobayashi, H., and Okuda, S. Studies on macrocyclic lactone antibiotics. XI. Anti-mitotic and anti-tubulin activity of new antitumor antibiotics, rhizoxin and its homologues. *J. Antibiotics*, *40*: 66-72, 1987.
  33. Christian, M. C., Pluda, J. M., Ho, P. T. C., Arbuck, S. G., Murgu, A. J., and Sausville, E. A. Promising new agents under development by the division of cancer treatment, diagnosis, and centers of the National Cancer Institute. *Semin. Oncol.*, *24*: 219-240, 1998.
  34. D'Ambrosio, M., Guerriero, A., and Pietra, F. Isolation from the mediterranean stoloniferan coral *Sarcodictyon roseum* of sarcodictyin C, D, E, and F, novel diterpenoidic alcohols esterified by (E)- or (Z)-N(1)-methylurocanic acid. Failure of the carbon-skeleton type as a classification criterion. *Helv. Chim. Acta*, *71*: 964-976, 1988.
  35. Ciomei, M., Albanese, C., Pastori, W., Grandi, M., Pietra, F., D'Ambrosio, M., Guerriero, A., and Battistini, C. Sarcodictyins: a new class of marine derivatives with mode of action similar to Taxol. *Proc. Am. Assoc. Cancer Res.*, *38*: 5, 1997.

36. Nicolaou, K. C., Kim, S., Pfefferkorn, J., Xu, J., Ohshima, T., Hosokawa, S., Vourloumis, D., and Li, T. Synthesis and biological activity of sarcyodictyins. *Angew. Chem. Int. Ed. Engl.*, *37*: 1418-1421, 1998.
37. McDaid, H. M., Bhattacharya, S. K., Chen, X.-T., He, L., Shen, H.-J., Gutteridge, C. E., Horwitz, S. B., and Danishefsky, S. J. Structure-activity profiles of eleutherobin analogs and their cross-resistance in Taxol-resistant cell lines. *Cancer Chemother. Pharmacol.*, *44*: 131-137, 1999.
38. Hamel, E., Sackett, D. L., Vourloumis, D., and Nicolaou, K. C. The coral-derived natural products eleutherobin and sarcodictyins A and B: effects on the assembly of purified tubulin with and without microtubule-associated proteins and binding at the polymer taxoid site. *Biochemistry*, *38*: 5490-5498, 1999.
39. ter Haar, E., Kowalski, R. J., Hamel, E., Lin, C. M., Longley, R. E., Gunasekara, S. P., Rosenkranz, H. S., and Day, B. W. Discodermolide, a cytotoxic marine agent that stabilizes microtubules more potently than taxol. *Biochemistry*, *35*: 243-250, 1996.
40. Bollag, D. M., McQueney, P. A., Zhu, J., Hensens, O., Koupal, L., Liesch, J., Goetz, M., Lazarides, E., and Woods, C. M. Epothilones, a new class of microtubule-stabilizing agents with a taxol-like mechanism of action. *Cancer Res.*, *55*: 2325-2333, 1995.
41. Mooberry, S. L., Tien, G., Hernandez, A. H., Plubrukarn, A., and Davidson, B. S. Laulimalide and isolaulimalide, new paclitaxel-like microtubule-stabilizing agents. *Cancer Res.*, *59*: 653-660, 1999.
42. Winkler, J. D. and Axelsen, P. H. A model for the taxol (paclitaxel)/epothilone pharmacophore. *Bioorg. Med. Chem. Lett.*, *6*: 2963-2966, 1996.
43. Wang, M., Xia, X., Kim, Y., Hwang, D., Jansen, J. M., Botta, M., Liotta, D. C., and Snyder, J. P. A unified and quantitative receptor model for the microtubule binding of paclitaxel and epothilone. *Organic Letters*, *1*: 43-46, 1999.

44. Ojima, I., Chakravarty, S., Inoue, T., Lin, S., He, L., Band Horwitz, S., Kuduk, S. D., and Danishefsky, S. J. A common pharmacophore for cytotoxic natural products that stabilize microtubules. *Proc. Natl. Acad. Sci. USA*, *96*: 4256-4261. 1999.
45. Wani, M. C., Taylor, H. L., Wall, M. E., Coggon, P., and McPhail, A. T. Plant antitumor agents, VI: The isolation and structure of Taxol, a novel antileukemic and antitumor agent from *Taxus brevifolia*. *J. Am. Chem.Soc.*, *93*: 2325-2327. 1971.
46. Baloglu, E. and Kingston, D. G. I. The taxane diterpenoids. *J. Nat. Prod.*, *62*: 1448-1472, 1999.
47. Rayl, A. J. S. Oceans: medicine chests of the future? *The Scientist*, *13*: 1-5, 1999.
48. Look, S. A., Fenical, W., Van Engen, D., and Clardy, J. Erythrolides: unique marine diterpenoids interrelated by a naturally occurring Di- $\pi$ -methane rearrangement. *J. Am. Chem. Soc.*, *106*: 5026-5027, 1984.
49. Kinzie, R. A. The zonation of West Indian gorgonians. *Bull. Mar. Sci.*, *23*: 93-115, 1973.
50. Goldberg, W. M. The ecology of the coral-octocoral communities off the Southeast Florida coast: geomorphology, species composition, and zonation. *Bull. Mar. Sci.*, *23*: 465-488, 1973.
51. Opresko, D. M. Abundance and distribution of shallow-water gorgonians in the area of Miami, Florida. *Bull. Mar. Sci.*, *23*: 535-558, 1973.
52. Li, J. Y., Strobel, G., Sidhu, R. H., Hess, W. M., and Ford, E. J. Endophytic taxol-producing fungi from bald cypress, *Taxodium distichum*. *Microbiology*, *142*: 2223-2226, 1996.
53. Strobel, G., Yang, X., Sears, J., Kramer, R., Sidhu, R. S., and W.M., H. Taxol from *Pestalotiopsis microspora*, an endophytic fungus of *Taxus wallachiana*. *Microbiology*, *142*: 435-440, 1996.
54. Strobel, G. A., Ford, E., Li, J. Y., Sears, J., Sidhu, R. S., and Hess, W. M. *Semiatoantlerium tepuiense* gen. nov., a unique epiphytic fungus producing taxol from the Venezuelan Guyana. *Syst. Appl. Microbiol.*, *22*: 426-433, 1999.

55. Gosmann, G., Guillame, D., Taketa, A. T. C., and Schenkel, E. P. Triterpenoid saponins from *Ilex paraguariensis*. J. Nat. Prod.. 58: 438-441, 1995.

Table 1 *Pilot ELISA screen of microbial extracts*

96-well plate	A405 <sup>a</sup>			
	positive extracts	negative extracts	negative control (no extract added)	positive control (nocodazole)
A	1.135 1.437	0.270±0.051 (n=86)	0.294±0.098 (n=4)	1.615±0.068 (n=4)
B	-	0.280±0.040 (n=88)	0.267±0.033 (n=4)	1.298±0.136 (n=4)
C	1.245	0.276±0.040 (n=87)	0.305±0.035 (n=4)	1.448±0.059 (n=4)

<sup>a</sup> Values shown are mean and SD of the number of measurements shown in brackets. The absorbance readings are raw data, not corrected for background caused by the microtiter plate and reagents.

Table 2 *ELICA screen of plant extracts*

96-well plate	A405 <sup>a</sup>			
	positive extracts	negative extracts	negative control (no extract added)	positive control (nocodazole)
97040140	2.141 2.366 2.181	0.731±0.346 (n=85)	0.752±0.047 (n=4)	2.379±0.057 (n=4)
97040141	-	0.651±0.198 (n=88)	0.712±0.048 (n=4)	1.555±0.113 (n=4)
97040143	2.313 1.421	0.558±0.240 (n=86)	0.558±0.046 (n=4)	1.681±0.030(n=4)

<sup>a</sup> Values shown are mean and SD of the number of measurements shown in brackets. The absorbance readings are raw data, not corrected for background caused by the microtiter plate and reagents.

## FIGURE LEGENDS

Fig. 1. Western blot, using the TG-3 antibody, of total protein extracts from cycling cells and nocodazole-treated cells (lanes 1, 2). Arrow indicates the mitotically phosphorylated form of nucleolin at 105 kDa. The film was overexposed to illustrate the quantitative difference between cells treated or not with the antimitotic agent. Coomassie blue-stained lanes used as gel loading controls (lanes 3, 4).

Fig. 2. Evaluation of the ELISA and ELICA assays using paclitaxel. A, B, cells were treated with different concentrations of paclitaxel for 20 h and antimitotic activity was determined using mitotic spreads (black circle), ELISA (open square), or ELICA (black squares). Experiments were carried out in triplicate and values indicate means  $\pm$  SD.

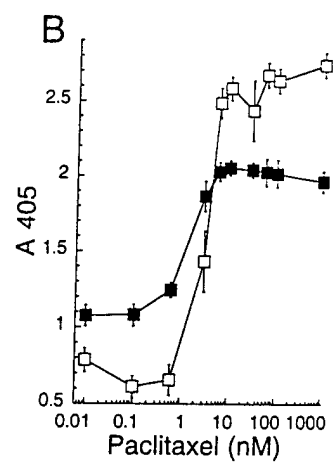
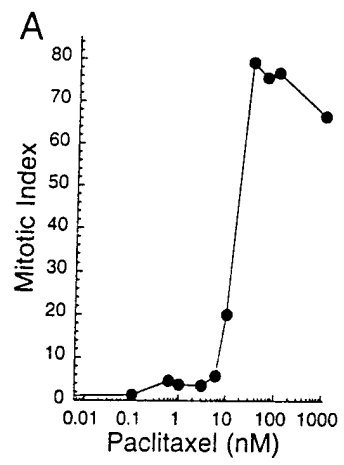
Fig. 3. Structural formulae of rhizoxin and analogs.

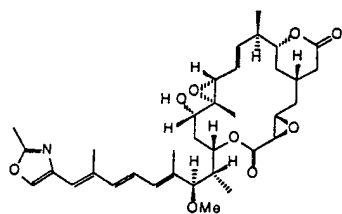
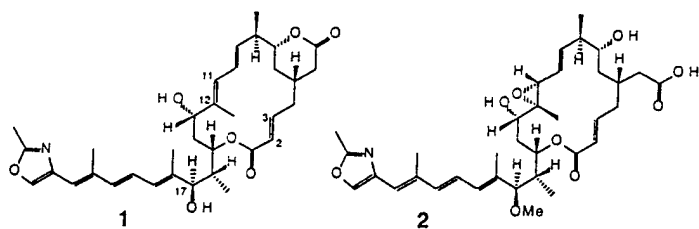
Fig. 4. Structural formulae of eleutherobin and analogs. The boxed regions A, B and C of eleutherobin are those considered important for activity in the pharmacophore proposed in (44).

Fig. 5. Antimitotic activity of eleutherobin and analogs. Cells were treated with different concentrations of the compounds for 20h and mitotic arrest was determined by ELICA. The absorbance values were transformed into % mitotic cells using a standard curve constructed by measuring the absorbance values of cell populations containing defined percentages of mitotic cells (18).

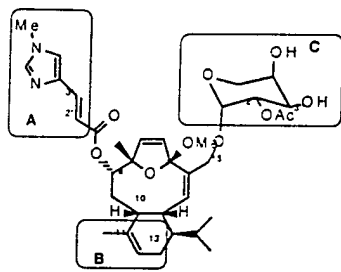
Fig. 6. Structural formulae of paclitaxel and analogs.



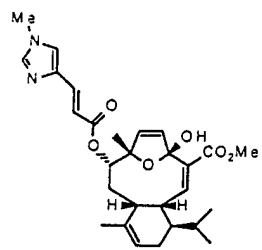




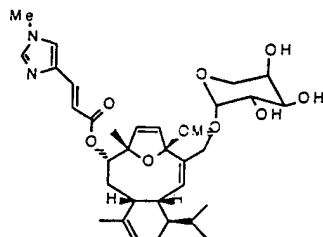
Rhizoxin



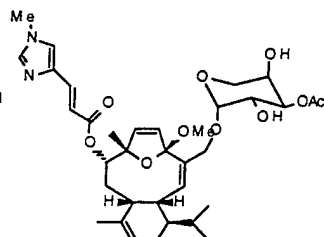
3 Eleutherobin



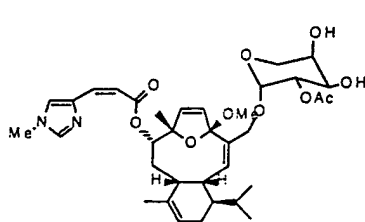
4 Sarcodictyin A



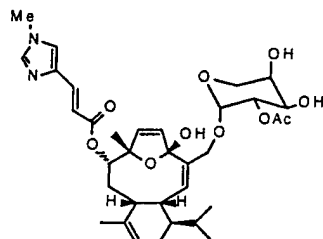
5 Desacetyeleutherobin



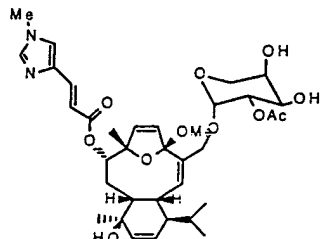
6 Isoeleutherobin



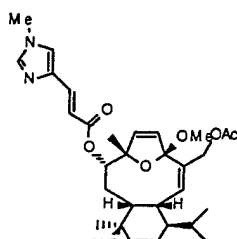
7 Z-Eleutherobin



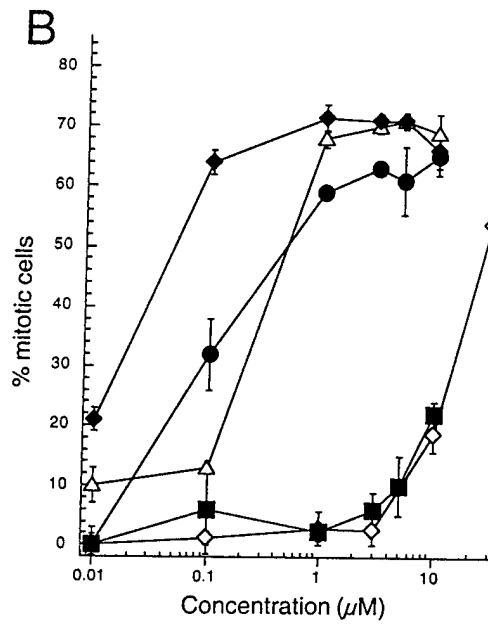
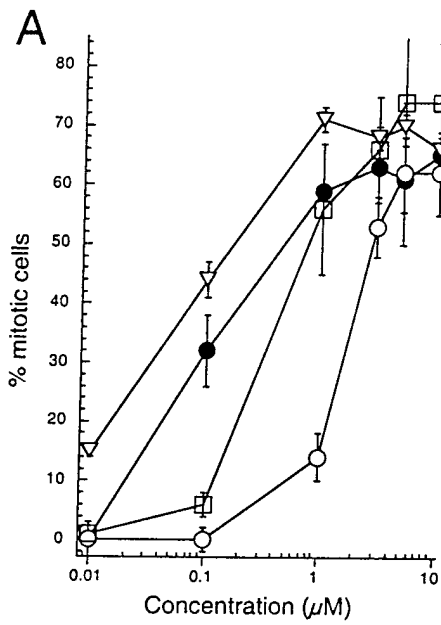
8 Desmethyleleutherobin



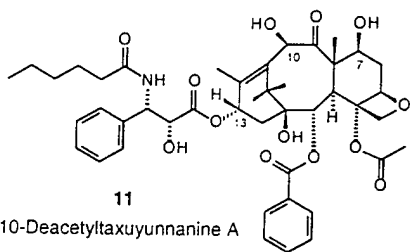
9 Caribaeoside



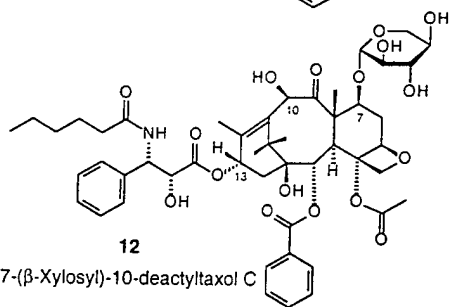
10 Caribaeolin



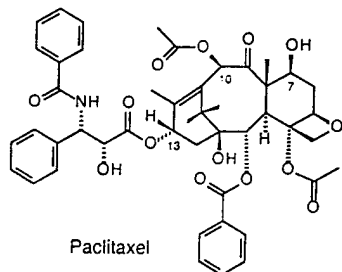
- Eleutherobin (3)
- Sarcodictyin A (4)
- Desacetylleutherobin (5)
- ▽ Isoeleutherobin A (6)
- △ Z-Eleutherobin (7)
- ◆ Desmethyleleutherobin (8)
- Caribaeoside (9)
- ◇ Caribaeolin (10)



11  
10-Deacetyltaxuyunnanine A



12  
7-(β-Xylosyl)-10-deactyltaxol C



Paclitaxel

# Antimitotic Diterpenes from *Erythropodium caribaeorum* Test Pharmacophore Models for Microtubule Stabilization

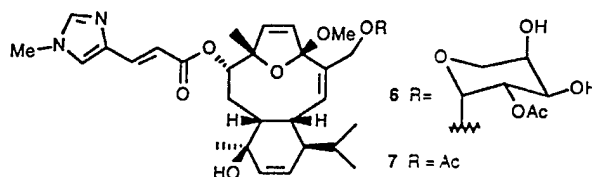
Bruno Cinel,<sup>†</sup> Michel Roberge,<sup>‡</sup> Hans Behrisch,<sup>§</sup> Leen van Ofwegen,<sup>||</sup>  
Clovis B. Castro,<sup>⊥</sup> and Raymond J. Andersen<sup>\*†</sup>

Departments of Chemistry and Oceanography (EOS), University of British Columbia,  
Vancouver, B.C., Canada, V6T 1Z1, Department of Biochemistry and Molecular  
Biology, University of British Columbia, Vancouver, B.C., Canada, V6T 1Z3, Ross  
University Medical School, Commonwealth of Dominica, Nationaal Natuurhistorisch  
Museum, Leiden, The Netherlands, and Museu Nacional, Rio de Janeiro, Brazil

randersn@unixg.ubc.ca

Received October 29, 1999

## ABSTRACT



Six new antimitotic diterpenes, 2-7, have been isolated from the Caribbean octocoral *Erythropodium caribaeorum*. Structural variations encountered in this group of natural products test recently proposed pharmacophore models for microtubule stabilizing compounds.

Antimitotic compounds interfere with the dynamic assembly and disassembly of  $\alpha$ - and  $\beta$ -tubulin into microtubules, causing cells to arrest in mitosis.<sup>1</sup> Prolonged arrest in mitosis eventually leads to cell death, mainly by apoptosis. Two chemical classes of antimitotic agents, the vinca alkaloids (vinblastine, vincristine, and vinorelbine) and the taxanes (paclitaxel and docetaxel), are clinically useful anticancer drugs. Most known antimitotic agents, including the vinca alkaloids, induce mitotic arrest by inhibiting the polymerization of tubulin into microtubules. Paclitaxel was the first chemical entity shown to cause mitotic arrest by stabilizing

microtubules against depolymerization. Since the initial discovery of paclitaxel's mechanism of action and its introduction into clinical use, there has been much interest in finding other chemical structural types that also stabilize microtubules. Four additional chemotypes that have paclitaxel-like effects have subsequently been identified. These include the myxobacterium metabolites epothilones A and B,<sup>2</sup> the marine sponge metabolites discodermolide,<sup>3</sup> laulimalide, and isolaulimalide,<sup>4</sup> and the soft coral metabolite eleutherobin.<sup>5</sup> Ojima et al. have recently proposed a common pharmacophore for the microtubule stabilizing compounds that effectively accommodates nonataxel, paclitaxel, disco-

<sup>†</sup> Departments of Chemistry and Oceanography (EOS), University of British Columbia.

<sup>‡</sup> Department of Biochemistry and Molecular Biology, University of British Columbia.

<sup>§</sup> Ross University Medical School.

<sup>||</sup> Nationaal Natuurhistorisch Museum.

<sup>⊥</sup> Museu Nacional.

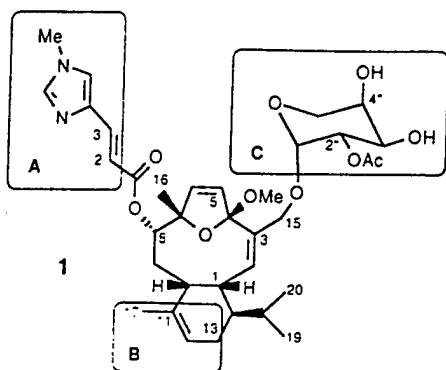
(1) (a) Jordan, A.; Hadfield, J. A.; Lawrence, N. J.; McGowen, A. T. *Med. Res. Rev.* 1998, 18, 259-296. (b) Hamel, E. *Ibid.* 1996, 16, 207-231.

(2) Bollag, D. M.; McQueney, P. A.; Zhu, J.; Hensens, O.; Koupal, L.; Liesch, J.; Goetz, M.; Lazarides, E.; Woods, C. M. *Cancer Res.* 1995, 55, 2325-2333.

(3) ter Haar, E.; Kowalski, R. J.; Hamel, E.; Lin, C. M.; Longley, R. E.; Gunasekera, S. P.; Rosenkranz, H. S.; Day, B. W. *Biochemistry* 1996, 35, 243-250.

(4) Mooberry, S. L.; Tien, G.; Hernandez, A. H.; Plubrukam, A.; Davidson, B. S. *Cancer Res.* 1999, 59, 653-660.

dermolide, eleutherobin, and the epothilones.<sup>6</sup> This model predicts that three regions of eleutherobin (**1**) (see boxes A, B, and C below) are important domains for binding to tubulin.

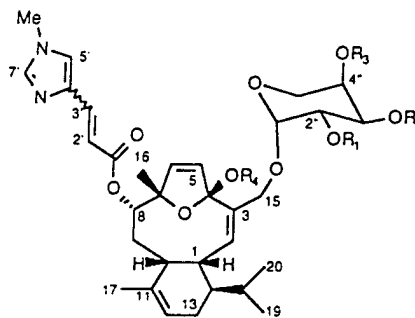


Most known antimitotic natural products were initially isolated because they exhibited potent *in vitro* cytotoxicity, and only subsequent mechanism of action studies revealed that they interfered with tubulin assembly and disassembly dynamics. Two classes of antimitotic agents, the epothilones<sup>2</sup> and the laulimalides,<sup>4</sup> have been discovered by rational screening, illustrating the significant potential for assay-directed identification of novel antimitotic chemotypes. Recently, a new cell-based antimitotic assay that is rapid and reliable has been developed in one of our laboratories.<sup>7</sup> Extracts of the octocoral *Erythropodium caribaeorum* collected at several sites in the Southern Caribbean showed potent activity in the assay.<sup>8</sup> Microscopic examination of cells arrested in mitosis by the *E. caribaeorum* extract showed evidence of tubulin bundling, similar to the effects of paclitaxel.

Bioassay guided fractionation of the *E. caribaeorum* extract led to the isolation of eleutherobin (**1**) and the new antimitotic diterpenoids desmethyleleutherobin (**2**), desacetyeleutherobin (**3**), isoeleutherobin A (**4**), Z-eleutherobin (**5**), caribaeoside (**6**), and caribaeolin (**7**). Compounds **3–7** all differ from eleutherobin in the proposed A, B, and C tubulin binding regions. In particular, caribaeoside (**6**) provides the first test for the B region in Ojima's model of the eleutherobin pharmacophore.

Freshly collected specimens of *E. caribaeorum* were frozen on site and transported to Vancouver over dry ice.

Thawed samples (5.3 kg wet wt) were extracted multiple times with MeOH, and the combined MeOH extracts were concentrated to a gum *in vacuo*. Fractionation of the crude gum (280 g) by sequential application of vacuum reversed-phase flash (gradient elution: 80:20 H<sub>2</sub>O/MeOH to MeOH in 10% increments), normal-phase flash (gradient elution: EtOAc to 80:20 EtOAc/MeOH in 2% increments), and normal-phase high-performance liquid chromatographies (eluent: 93:7 CH<sub>2</sub>Cl<sub>2</sub>/MeOH) gave pure samples of **1** (50 mg), **2** (7 mg), **3** (6 mg), **4** (3 mg), and **5** (2 mg). Compounds **6** (1 mg) and **7** (1 mg) partially decomposed on silica gel so they were isolated using only vacuum reversed-phase flash chromatography and cyano-bonded-phase HPLC (eluent: 56:42:2 EtOAc/hexane/(<sup>4</sup>Pr)<sub>2</sub>NH).



- 2 R<sub>1</sub> = Ac; R<sub>2</sub> = R<sub>3</sub> = R<sub>4</sub> = H; Δ<sup>2',3'</sup> (E)  
 3 R<sub>1</sub> = R<sub>2</sub> = R<sub>3</sub> = H; R<sub>4</sub> = Me; Δ<sup>2',3'</sup> (E)  
 4 R<sub>1</sub> = R<sub>3</sub> = H; R<sub>2</sub> = Ac; R<sub>4</sub> = Me; Δ<sup>2',3'</sup> (E)  
 5 R<sub>1</sub> = Ac; R<sub>2</sub> = R<sub>3</sub> = H; R<sub>4</sub> = Me; Δ<sup>2',3'</sup> (Z)  
 8 R<sub>1</sub> = R<sub>2</sub> = R<sub>3</sub> = Ac; R<sub>4</sub> = Me; Δ<sup>2',3'</sup> (E)

All NMR data for the *E. caribaeorum* diterpenes were recorded in DMSO-*d*<sub>6</sub> at 500 MHz. Tables of the NMR assignments are available in the Supporting Information. Eleutherobin (**1**) was identified by comparison of its spectroscopic data with literature values.<sup>5a</sup> Desmethyleleutherobin (**2**) was isolated as a clear oil that gave a [M + H]<sup>+</sup> ion in the HRFABMS at *m/z* 643.32230, appropriate for a molecular formula of C<sub>34</sub>H<sub>46</sub>N<sub>2</sub>O<sub>10</sub> (ΔM -1.21 ppm), that differed from the molecular formula of eleutherobin simply by the loss of CH<sub>2</sub>. The <sup>1</sup>H NMR spectrum of **2** differed from the <sup>1</sup>H NMR spectrum of eleutherobin (**1**) only by the absence of a methyl resonance at ~δ 3.1 that could be assigned to the C-4 methoxyl substituent. This evidence indicated that **2** was identical to eleutherobin (**1**) except for the presence of a hydroxyl group instead of a methoxyl group at C-4. The 2D NMR data obtained for **2** was in complete agreement with this assignment.

Desacetyeleutherobin (**3**) was isolated as a clear oil that gave a [M + H]<sup>+</sup> ion at *m/z* 615.32813 in the HRFABMS corresponding to a molecular formula of C<sub>33</sub>H<sub>46</sub>N<sub>2</sub>O<sub>9</sub> (ΔM -0.05 ppm), which differed from the formula of eleutherobin (**1**) by the loss of C<sub>2</sub>H<sub>2</sub>O. The <sup>1</sup>H NMR spectrum of **3** showed a strong resemblance to the <sup>1</sup>H NMR spectrum of eleutherobin (**1**) except for the absence of a methyl singlet at ~δ 2 that could be assigned to an acetyl residue and the chemical shifts of the resonances assigned to the arabinose protons. These NMR differences suggested that **3** was simply the

(5) (a) Lindel, T.; Jensen, P. R.; Fenical, W.; Long, B. H.; Casazza, A. M.; Carboni, J.; Fairchild, C. R. *J. Am. Chem. Soc.* 1997, 119, 8744–8745. (b) Long, B. H.; Carboni, J. M.; Wasserman, A. J.; Cornell, L. A.; Casazza, A. M.; Jensen, P. R.; Lindel, T.; Fenical, W.; Fairchild, C. R. *Cancer Res.* 1998, 58, 1111–1115. (c) Hamel, E.; Sackett, D. L.; Vourloumis, D.; Nicolaou, K. C. *Biochemistry* 1999, 38, 5490–5498.

(6) Ojima, I.; Chakravarty, S.; Inoue, T.; Lin, S.; He, L.; Horwitz, S. W.; Kuduk, S. D.; Danishefsky, S. J. *Proc. Natl. Acad. Sci. U.S.A.* 1999, 96, 4256–4261.

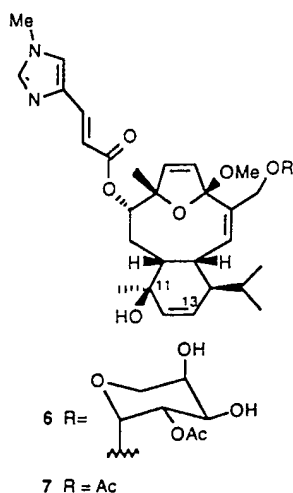
(7) Roberge, M.; Cinel, B.; Anderson, H.; Lim, L.; Jiang, X.; Xu, L.; Kelly, M. T.; Andersen, R. J. *Cancer Res.* Submitted for publication.

(8) For previous chemical studies of *E. caribaeorum*, see: (a) Maharaj, D.; Pascoe, K. O.; Tinto, W. F. *J. Nat. Prod.* 1999, 62, 313–314. (b) Athirana, C.; Fenical, W. F.; Corcoran, E.; Clardy, J. *Tetrahedron Lett.* 1993, 34, 3371–3372. (c) Pordesimo, E. O.; Schmitz, F. J.; Ciereszko, L.; Hossain, M. B.; Van der Helm, D. *J. Org. Chem.* 1991, 56, 2344–2357. (d) Look, S. A.; Fenical, W. F.; Van Engen, D.; Clardy, J. *J. Am. Chem. Soc.* 1984, 106, 5026–5027.

desacetyl analogue of eleutherobin (1). Acetylation of 3 with acetic anhydride in pyridine converted it to diacetyeleutherobin (8), which was identical to 8 prepared by acetylation of eleutherobin using the same reaction conditions, confirming the proposed structure of 3.

Isoeleutherobin A (4), isolated as a clear oil, gave an  $[M + H]^+$  ion at  $m/z$  657.33834 in the HRFABMS corresponding to a molecular formula of  $C_{35}H_{48}N_2O_{10}$  ( $\Delta M$  -0.58 ppm), which was identical to the molecular formula of eleutherobin (1). Comparison of the  $^1H$  1D and 2D NMR data for isoeleutherobin A (4) with the data for eleutherobin (1) showed that the molecules differed only in the position of acetylation on the arabinose fragment. COSY correlations observed between resonances at  $\delta$  3.38 and 3.62 (both broad doublets:  $J = 12.2$  Hz), assigned to the C-5'' methylene protons, and a methine at  $\delta$  3.83 (H-4'': m) showed that the acetate was not at C-4''. The H-4'' resonance in turn showed a COSY correlation to a resonance at  $\delta$  4.80 (dd,  $J = 2.5, 10.1$  Hz), assigned to H3'', which was significantly deshielded relative to the corresponding H3'' resonance ( $\delta$  3.73) in eleutherobin (1). Therefore, isoeleutherobin A was assigned structure 4. Acetylation with acetic anhydride in pyridine converted isoeleutherobin A (4) to diacetyeleutherobin (8), confirming the assigned structure of 4.

Z-Eleutherobin (5) gave a  $[M + H]^+$  ion at  $m/z$  657.33830 in the HRFABMS appropriate for a molecular formula of  $C_{35}H_{48}N_2O_{10}$  ( $\Delta M$  -0.65 ppm), again identical to the molecular formula of eleutherobin (1). Comparison of the NMR data obtained for 5 with the data for 1 showed that the molecules differed only in the configuration of the  $\Delta^{2,3}$  olefin. In the  $^1H$  NMR spectrum of Z-eleutherobin (5), the uroconic acid olefinic proton resonances appeared at  $\delta$  5.75 (H-2') and 6.94 (H-3') with a coupling constant of 12.6 Hz, whereas in the spectrum of eleutherobin (1) they were found at  $\delta$  6.35 (H-2') and 7.53 (H-3') with a coupling constant of 15.6 Hz. The NMR sample of Z-eleutherobin (5) partially isomerized over time to eleutherobin (1), confirming the assigned structure.



Caribaeoside (6), obtained as a colorless glass, gave a  $[M + H]^+$  ion in the HRFABMS at  $m/z$  673.33474 appropriate for a molecular formula of  $C_{35}H_{48}N_2O_{11}$  ( $\Delta M$  1.64 ppm),

that only differed from the molecular formula of eleutherobin (1) by the presence of one additional oxygen atom. Analysis of the NMR data obtained for caribaeoside (6) revealed that it too was a diterpene glycoside with the same *N*-(6')-methyluroconic acid and 2''-*O*-acetyl arabinose substituents that are attached to the central core of eleutherobin (1).

A number of features of the NMR data revealed that caribaeoside (2) and eleutherobin (1) differed in the C-11 to C-13 regions of their diterpene cores. The C-17 olefinic methyl resonance at  $\delta$  1.47 and the H-12 olefinic methine resonance at  $\delta$  5.27 in the  $^1H$  NMR spectrum of eleutherobin (1) were both missing in the  $^1H$  NMR spectrum of caribaeoside (6). In their place, the  $^1H$  NMR spectrum of 6 had a singlet methyl resonance at  $\delta$  0.82 and a pair olefinic methine resonances at  $\delta$  5.52–5.54 (H-12 and H-13). The two-proton olefinic resonance showed correlations in the HMQC spectrum to carbon resonances at  $\delta$  125.6 (C-13) and 137.4 (C-12). HMBC correlations observed between the Me-17 singlet at  $\delta$  0.82 and the C-12 olefinic resonance at  $\delta$  137.4, a quaternary carbon resonance at  $\delta$  68.3, and a methine resonance at  $\delta$  45.7 (HMQC to  $\delta$  2.07) confirmed the proximity of Me-17 and C-12 and indicated that there was a hydroxyl substituent at C-11 and a methine carbon at C-10.<sup>9</sup> A pair of overlapping doublets (6H) at  $\delta$  0.94–0.95, that showed COSY correlations to a methine resonance at  $\delta$  1.68, were assigned to the Me-19 and Me-20 isopropyl protons, and a multiplet at  $\delta$  4.00, that showed COSY correlations to an olefinic doublet at  $\delta$  5.38 (H-2) and a methine resonance at  $\delta$  2.07 (H-10), was assigned to H-1. The H-1 resonance in the spectrum of 6 had a chemical shift and multiplicity nearly identical to the H-1 resonance in eleutherobin (1) ( $\delta$  3.88), consistent with the proposal that the C-1, C-2, C-10, and C-14 centers in 6 were identical to the corresponding sites in 1.

ROESY and scalar coupling constant data established the relative stereochemistry about the cyclohexene ring in caribaeoside (6). The resonances assigned to H-1 ( $\delta$  4.00) and H-2 ( $\delta$  5.38) in 6 had chemical shifts and a vicinal coupling constant ( $J = 9.7$  Hz) nearly identical with their counterparts in eleutherobin (1) ( $\delta$  H-1, 3.88; H-2, 5.39;  $J = 9.4$  Hz), indicating that the dihedral angle between them in 6 was essentially identical to that in 1. ROESY correlations observed between the isopropyl methyl proton resonances at  $\delta$  0.94–0.95 and the H-1 ( $\delta$  4.00) and H-10 ( $\delta$  2.07) resonances in 6, demonstrated that the isopropyl group, H-1, and H-10 were on the same face of the molecule, as in eleutherobin (1). The Me-17 resonance at  $\delta$  0.82 in 6 showed a strong ROESY correlation to the H-2 ( $\delta$  5.38) resonance demonstrating that Me-17 and C-2 were *cis*. Models indicate that the Me-17 protons can sit in the shielding region of the  $\Delta^{2,3}$  olefin, consistent with their unusually shielded chemical shift of  $\delta$  0.82. ROESY correlations observed between Me-16 ( $\delta$  1.33) and both H-8 ( $\delta$  4.85) and OMe-21 ( $\delta$  3.08), and between H-8 and H-10 ( $\delta$  2.07), confirmed that car-

(9) Sarcodictyin F, a related 4,7-oxaunicellane diterpenoid, has a similarly functionalized cyclohexene ring, but with the opposite stereochemistry at C-11. See: D'Ambrosio, M.; Guerriero, A.; Pietra, F. *Helv. Chim. Acta* 1988, 71, 964–976.

ibaeside (6) and eleutherobin (1) had identical relative stereochemistries at C-4, C-7, C-8, and C-10.

Caribaeolin (7) was isolated as a clear oil that gave a  $[M + H]^+$  ion in the HRFABMS at  $m/z$  541.29111 corresponding to a molecular formula of  $C_{30}H_{40}N_2O_7$  ( $\Delta M$  -0.49 ppm). Analysis of the 1D and 2D  $^1H$  detected NMR data obtained for 7 revealed that it contained the diterpene core and *N*-(6')-methyluroconic acid fragments that constitute the aglycon of caribaeoside (6) but was missing the arabinose sugar residue. COSY and ROESY correlations were observed between an olefinic methine resonance at  $\delta$  5.38, assigned to H-2, and a broad two proton singlet at  $\delta$  4.46, assigned to the H-15 methylene protons. HMBC correlations were observed between a carbonyl resonance at  $\delta$  169.9 and both the H-15 methylene proton resonance at  $\delta$  4.46 and a singlet methyl resonance at  $\delta$  1.97. These HMBC correlations demonstrated that in caribaeolin (7) a C-15 acetyl substituent was present in place of the C-15 arabinose sugar residue found in caribaeoside (6). Strong ROESY correlations were observed between the Me-17 resonance at  $\delta$  0.77 and the H-2 olefinic proton resonance at  $\delta$  5.38, indicating that Me-17 and C-2 were *cis* to each other as in caribaeoside (6). Additional ROESY correlations observed between the C-19/C-20 isopropyl methyl proton resonances at  $\delta$  0.95–0.96 and the H-1 ( $\delta$  4.01) and H-10 ( $\delta$  2.07) resonances, between the Me-16 ( $\delta$  1.34) and both of the H-8 ( $\delta$  4.85) and OMe-21 ( $\delta$  3.08) resonances, and between the H-8 and H-10 ( $\delta$  2.07) resonances confirmed that the relative stereochemistry in caribaeolin (7) was the same as in caribaeoside (6).

All of the *E. caribaeorum* diterpenoids 1–7 reported above showed antimittotic activity in the cell-based assay.<sup>7</sup> Desmethyleneleutherobin (2) ( $IC_{50}$  20 nM) and isoeleutherobin A (4) ( $IC_{50}$  50 nM) were both slightly more potent than eleutherobin (1) ( $IC_{50}$  100 nM), *Z*-eleutherobin (5) ( $IC_{50}$  250 nM) was comparable in activity to eleutherobin (1), des-acetyeleutherobin (3) ( $IC_{50}$  400 nM) was slightly less potent, while caribaeoside (6) ( $IC_{50}$  20  $\mu M$ ) and caribaeolin (7) ( $IC_{50}$  20  $\mu M$ ) were considerably less potent than eleutherobin (1).

Many synthetic analogues of eleutherobin (1) have been prepared as part of SAR studies;<sup>10</sup> however, to date they have

all been based on the eleutherobin diterpenoid core. The Ojima pharmacophore proposal implies that changes in the C-11–C-13 region of eleutherobin should have an impact on the ability of analogues to stabilize tubulin polymers. Caribaeoside (6) represents the first such analogue to be tested for antimittotic activity. The significant decrease in antimittotic potency of caribaeoside (6) relative to eleutherobin (1), resulting from introduction of a hydroxyl group at C-11 and migration of the olefin to the  $\Delta^{12,13}$  position, provides further support for Ojima's pharmacophore model. The structural changes in 6 alter both the shape and polarity of the diterpene core in the tubulin binding region B of the proposed pharmacophore.

A number of other features of the antimittotic potencies are also noteworthy. Altering the  $\Delta^{2,3'}$  configuration (i.e., 5), a change in the A region of the pharmacophore, has little effect, while alterations in the arabinose fragment, representing changes in the C region of the pharmacophore, can either enhance (i.e., 4) or decrease (i.e., 3) the potency. Changing the C-4 substituent from methoxyl (i.e., 1) to hydroxyl (i.e., 2), an alteration that is formally outside of the Ojima pharmacophore binding regions, leads to a slight increase in potency. Replacement of the arabinose fragment in caribaeoside (6) with a simple acetate residue (i.e., 7) results in no additional loss of potency, which is consistent with previous observations.<sup>6</sup>

In summary, the current study has identified a new and relatively high-yielding source of eleutherobin (1), whose preclinical development has been impeded by its scarcity, as well as providing a series of new eleutherobin analogues 2–7 that serve as a further test of recent pharmacophore models for microtubule stabilization.

**Acknowledgment.** Financial support was provided by the National Cancer Institute of Canada (R.J.A.), NSERC (R.J.A.), and the Canadian Breast Cancer Research Initiative (M.R.). The authors thank M. LeBlanc, D. Williams, R. Britton, and the staff of Ross University for assistance collecting the samples.

**Supporting Information Available:** Tables of optical rotations, UV data, and  $^1H$  and  $^{13}C$  NMR assignments for compounds 1–8. This material is available free of charge via the Internet at <http://pubs.acs.org>.

OL9912027

(10) (a) McDaid, H. M.; Bhattacharya, Chen, X.-T.; He, L.; Shen, H.-J.; Gutteridge, C. E.; Horowitz, S. B.; Danishefsky, S. J. *Cancer Chemother. Pharmacol.* 1999, 44, 131–137. (b) Nicolaou, K. C.; Winssinger, N.; Vourloumis, D.; Ohshima, T.; Kim, S.; Pfeifferkorn, J.; Xu, J.-Y.; Li, T. *J. Am. Chem. Soc.* 1998, 120, 10814–10826.



Pergamon

Tetrahedron Letters 41 (2000) 2811–2815

TETRAHEDRON  
LETTERS

## Solid-state and solution conformations of eleutherobin obtained from X-ray diffraction analysis and solution NOE data

Bruno Cinel,<sup>a</sup> Brian O. Patrick,<sup>b</sup> Michel Roberge<sup>c</sup> and Raymond J. Andersen<sup>a,\*</sup>

<sup>a</sup>Departments of Chemistry and Earth and Ocean Sciences, University of British Columbia, Vancouver BC V6T 1Z1, Canada

<sup>b</sup>Department of Chemistry, University of British Columbia, Vancouver BC V6T 1Z1, Canada

<sup>c</sup>Department of Biochemistry and Molecular Biology, University of British Columbia, Vancouver BC V6T 1Z3, Canada

Received 22 January 2000; accepted 4 February 2000

### Abstract

Single crystal X-ray diffraction analysis has revealed the solid-state conformation of the microtubule-stabilizing diterpenoid eleutherobin (**1**). NOE data obtained for **1** in CDCl<sub>3</sub> and DMSO-*d*<sub>6</sub> are consistent with solution conformations that are virtually identical to the solid state conformation. © 2000 Elsevier Science Ltd. All rights reserved.

Eleutherobin (**1**), initially isolated from a Western Australian octocoral in the genus *Eleutherobia* (possibly *albiflora*), represents one of a small number of antimitotic natural product families that are known to stabilize microtubules.<sup>1</sup> Other structural types possessing this important biological activity are represented by paclitaxel,<sup>2</sup> epothilones A and B,<sup>3</sup> discodermolide,<sup>4</sup> and the laulimalides.<sup>5</sup> The current excitement surrounding this group of compounds stems from the FDA approval of paclitaxel for the treatment of ovarian (1992) and metastatic breast cancers (1994). Paclitaxel's clinical utility has generated great interest in developing additional anticancer drug candidates that exploit its mechanism of action. One approach to designing the next generation of microtubule-stabilizing compounds has been to create three-dimensional pharmacophore models that embrace all the available SAR data for the known natural product structural types with these properties.<sup>6,7</sup> The validity of this approach has been demonstrated by the pharmacophore-guided design and subsequent synthesis of new hybrid structures with demonstrated cytotoxic and tubulin binding abilities.<sup>6</sup>

Creation of predictive pharmacophore models depends on detailed knowledge about the conformation of all the known structural types possessing microtubule stabilizing properties. To date, there have been no published solid-state or solution conformational analyses of eleutherobin (**1**), although the original report of the structure elucidation did provide a series of useful NOE constraints. Recently, we discovered that the Caribbean octocoral *Erythropodium caribaeorum* is a relatively high-yielding source

\* Corresponding author. Tel: 604 822 4511; Fax: 604 822 6091; e-mail: randersn@unixg.ubc.ca (R. J. Andersen)

of eleutherobin and several new structural analogs.<sup>8</sup> During the course of characterizing the antimittotic diterpenes from the *E. caribaeorum* extracts, several crystals of eleutherobin (1) were obtained by the fortuitous slow evaporation of a concentrated NMR sample dissolved in DMSO-*d*<sub>6</sub>. The crystals proved to be suitable for X-ray diffraction analysis, which has provided the first solid state conformation for eleutherobin (1). ROESY and difference NOE data have also been collected for eleutherobin (1) in DMSO-*d*<sub>6</sub> and CDCl<sub>3</sub> in order to facilitate a comparison of the solid state conformation with the solution conformations in both a polar and a nonpolar solvent.

Eleutherobin (1) crystallized in space group  $P2_12_12_1$  with  $a=12.8291(8)$ ,  $b=13.6209(6)$ , and  $c=19.168(1)$  Å. A crystal with dimensions 0.30×0.20×0.15 mm, was mounted on a glass fiber. Data were collected at -100°C on a Rigaku/ADSC CCD area detector in two sets of scans ( $\phi=0.0$  to 190.0°,  $\chi=0^\circ$ ; and  $\omega=-18.0$  to 23.0°,  $\chi=-90^\circ$ ) using 0.50° oscillations with 58.0 s exposures. The crystal-to-detector distance was 40.55 mm with a detector swing angle of -5.52°. Of the 7035 unique reflections measured (Mo-K $\alpha$  radiation,  $2\theta_{\max}=55.8^\circ$ ,  $R_{int}=0.071$ , Friedels not merged), 4520 were considered observed ( $I>3\sigma(I)$ ). The final refinement residuals were  $R=0.046$  (on  $F$ ,  $I>3\sigma(I)$ ) and  $wR2=0.141$  (on  $F^2$ , all data).<sup>9</sup> The data was processed using the d\*TREK program and corrected for both Lorentz and polarization effects. The structure was solved by direct methods<sup>10</sup> and all non-hydrogen atoms were refined anisotropically, while all hydrogens involved in hydrogen-bonding were refined isotropically. All other hydrogens were included in calculated positions. The enantiomorph shown in Fig. 1 was chosen based on the known configuration of eleutherobin (1).<sup>11</sup> All calculations were performed using the teXsan<sup>12</sup> crystallographic software package of the Molecular Structure Corporation.

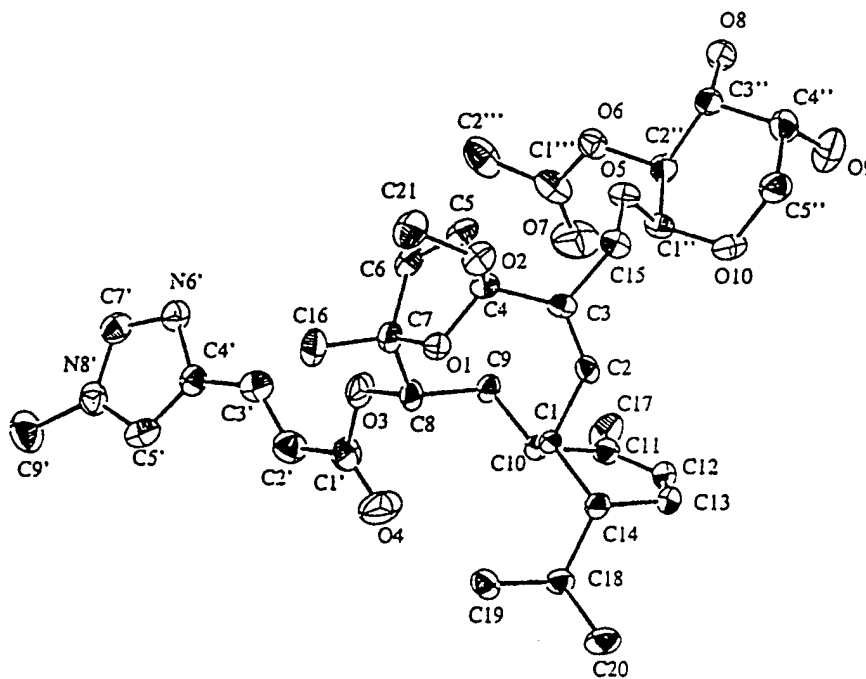


Fig. 1. ORTEP drawing of eleutherobin (1). Hydrogen atoms have been omitted for clarity

ROESY (500 MHz) and difference NOE (400 MHz) data were collected for eleutherobin (1) dissolved in DMSO-*d*<sub>6</sub> and CDCl<sub>3</sub>. The NMR samples were degassed and purged of oxygen by freezing in a dry ice/acetone bath and placing the frozen sample under vacuum. The degassed samples were then flushed with argon and sealed. Table 1 lists the difference NOE results obtained in CDCl<sub>3</sub> and the ROESY

correlations observed in  $\text{CDCl}_3$  and  $\text{DMSO}-d_6$  along with the solid-state internuclear distances between the relevant pairs of protons. A number of key NOEs indicate that the solution conformation of the diterpenoid core of eleutherobin (1) in both  $\text{CDCl}_3$  and  $\text{DMSO}-d_6$  is identical to, or at least extremely similar to, the solid state conformation. These include difference NOEs observed in the resonances for H1, H10, and Me19 when the H8 resonance is irradiated and in H13 $\alpha$  when H2 is irradiated. The C8-C9-C10-C1 torsional angle in the solid state is  $-66^\circ$ , which places H8 2.438 Å from H1 and 2.304 Å from H10, consistent with the difference NOEs observed. A C9-C10-C1-C14 torsional angle of  $177.7^\circ$  in the solid state brings the Me19 protons into sufficient proximity to H8 to explain the weak difference NOE observed between their resonances, and the C2-C1-C14-C13 torsional angle of  $-61^\circ$  in the solid state places H2 only 2.118 Å from H13 $\alpha$  in agreement with the strong difference NOE observed between their resonances. Molecular models indicate that the combination of H8 to H10, H1, Me19 and H2 to H13 $\alpha$  NOEs represent an extremely restrictive set of conformational constraints. Any significant deviation from the solid-state conformation results in H8 to H1, H10, Me19 and H2 to H13 $\alpha$  interproton distances that would make the simultaneous appearance of the observed suite of NOEs between these protons highly unlikely. The diagnostic dipolar couplings between H8 and both H1 and H10, and between H2 and H13 $\alpha$ , are all observed as ROESY correlations in both  $\text{CDCl}_3$  and  $\text{DMSO}-d_6$ , providing additional evidence that the solution conformations in both solvents must be essentially identical to the solid-state conformation.

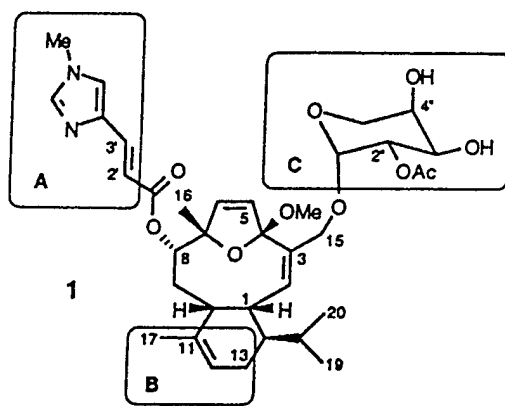
Table 1  
Difference NOE<sup>a</sup> and ROESY<sup>b</sup> data for eleutherobin (1) in  $\text{CDCl}_3$  and  $\text{DMSO}-d_6$

H# ( $\delta$ in $\text{CDCl}_3$ )	H# ( $\delta$ in $\text{CDCl}_3$ )	Internuclear Distance from X- ray Data (Å)	Difference NOE (% enhancement) H in First Column was Irradiated	ROESY Correlations in $\text{CDCl}_3$	ROESY Correlations in $\text{DMSO}-d_6$
H2 (5.54)	H13 $\alpha$ (2.29) <sup>c</sup>	2.12	7.49	y	y
H2	H14 (1.21)	2.61	3.51	y	y
H8 (4.80)	H1 (3.94)	2.44	4.28	y	y
H8	H10 (2.60)	2.30	6.16	y	y
H8	H16 (1.43)	2.52	0.91	y	y
H8	H19 (0.96)	2.64	0.52	y	n
H10 (2.60)	H1 (3.94)	2.33	4.79	y	y
H10	H8 (4.80)	2.30	2.61	y	y
H10	H19 (0.96)	2.51	0.77	n	n
H13 $\alpha$ (2.29) <sup>c</sup>	H2 (5.54)	2.12	9.69	y	y
H14 (1.21)	H1 (3.94)	2.37	6.40	y	y
H19 (0.96)	H1	2.02	0.97	y	y
H19	H8 (4.80)	2.64	0.32	y	n
H19	H10 (2.60)	2.51	0.42	n	n
H20 (0.94)	H13 $\beta$ (1.97) <sup>c</sup>	2.03	0.96	y	y
OMe (3.20)	H16 (1.43)	2.28	1.01	y	y

<sup>a</sup> 400 MHz; <sup>b</sup> 500 MHz; <sup>c</sup>  $\beta$  and  $\alpha$  are defined as being above and below the plane of the diterpenoid core of eleutherobin in the structural representation 1; n - ROESY correlation not clear; y - ROESY correlation clearly observed.

It is interesting to compare the conformation of eleutherobin (1) revealed by the X-ray diffraction and solution NOE data in the current study to the conformation used by Ojima et al. in constructing their common pharmacophore for microtubule-stabilizing natural products.<sup>6</sup> In order to generate a

conformation for pharmacophore creation, Ojima et al. carried out molecular dynamic calculations on eleutherobin (**1**) without using any constraints. The exact coordinates for the resulting conformation that they used for **1** were not available, but Figure 4 in their paper indicates that the modeled conformation had a C8–C9–C10–C1 torsional angle of  $>-90^\circ$  and a C2–C1–C14–C13 torsional angle approaching  $180^\circ$ . A conformation with those torsional angles would not be expected to give any of the NOEs that are observed between H8 and H1 and Me19, or between H2 and H13 $\alpha$  in CDCl<sub>3</sub> and DMSO-*d*<sub>6</sub>. The Ojima conformation gives their binding region B (C11–C12–C13) a much different spatial relationship relative to the A (uroconic acid side chain) and C (D-arabinose residue) binding regions compared to the solid-state conformation (see Scheme 1). This suggests that the solid-state and solution conformations of eleutherobin (**1**) determined herein might have significantly different overlay fits with the reference structure nonataxel and the other microtubule-stabilizing structures that were used to construct the common pharmacophore. Therefore, it is anticipated that the availability of solid-state and solution conformation data for eleutherobin (**1**) will facilitate further refinements of microtubule-stabilizing pharmacophore models and, consequently, aid the eventual design of new compounds with this important biological activity.



Scheme 1.

### Acknowledgements

Financial support was provided by the Natural Sciences and Engineering Research Council of Canada (R.J.A.), the National Cancer Institute of Canada (R.J.A.), the Canadian Breast Cancer Research Initiative (M.R.), and the US Department of Defense Breast Cancer Program Idea Award No. DAMD17-99-1-9088 (M.R.).

### References

- (a) Lindel, T.; Jensen, P. R.; Fenical, W.; Long, B. H.; Casazza, A. M.; Carboni, J.; Fairchild, C. R. *J. Am. Chem. Soc.* **1997**, *119*, 8744–8745. (b) Long, B. H.; Carboni, J. M.; Wasserman, A. J.; Cornell, L. A.; Casazza, A. M.; Jensen, P. R.; Lindel, T.; Fenical, W.; Fairchild, C. R. *Cancer Res.* **1998**, *58*, 1111–1115.
- Baloglu, E.; Kingston, D. G. I. *J. Nat. Prod.* **1999**, *62*, 1448–1472.
- Bollag, D. M.; McQueney, P. A.; Zhu, J.; Hensens, O.; Koupal, L.; Liesch, J.; Geotz, M.; Lazarides, E.; Woods, C. M. *Cancer Res.* **1995**, *55*, 2325–2333.

4. ter Haar, E.; Kowalski, R. J.; Hamel, E.; Lin, C. M.; Longley, R. E.; Gunasekera, S. P.; Rosenkranz, H. S.; Day, B. W. *Biochemistry* **1996**, *35*, 243–250.
5. Mooberry, S. L.; Tien, G.; Hernandez, A. H.; Plubrukarn, A.; Davidson, B. S. *Cancer Res.* **1999**, *59*, 653–660.
6. Ojima, I.; Chakravarty, S.; Inoue, T.; Lin, S.; He, L.; Horwitz, S. W.; Kuduk, S. D.; Danishefsky, S. J. *Proc. Natl. Acad. Sci., USA* **1999**, *96*, 4256–4261.
7. Wang, W.; Xia, X.; Kim, Y.; Hwang, D.; Jansen, J. M.; Botta, M.; Liotta, D. C.; Snyder, J. P. *Org. Lett.* **1999**, *1*, 43–46.
8. Cinel, B.; Roberge, M.; Behrisch, H.; van Ofwegen, L.; Castro, C. B.; Andersen, R. J. *Org. Lett.* **2000**, *2*, 257–260.
9. Archival crystallographic data have been deposited with the Cambridge Crystallographic Data Centre, University Chemical Laboratory, Lensfield Road, Cambridge CB2 1EW, UK. Please give a complete literature citation when ordering.
10. Altomare, A.; Cascarano, M.; Giacovazzo, C.; Guagliardi, A. *J. Appl. Cryst.*, **1993**, *26*, 343–350.
11. Chen, X.-T.; Bhattacharya, S. K.; Zhou, B.; Gutteridge, C. E.; Pettus, T. R. R.; Danishefsky, S. J. *J. Am. Chem. Soc.* **1999**, *121*, 6563–6579.
12. Crystal Structure Analysis Package, Molecular Structure Corporation (1985 and 1992).